

Role of Geophysical Testing in Geotechnical Site Characterization

M. Jamiolkowski

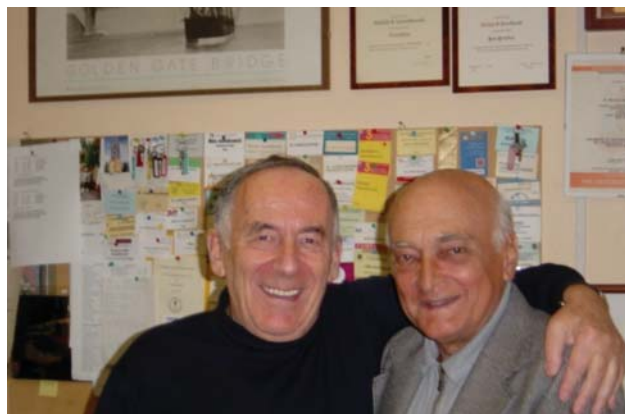
Abstract. The lecture attempts to highlight the insights late Victor De Mello provided on some key areas. Considering the increasing role of the geophysical methods in the geotechnical site characterization, the writer focuses on the use of in-hole geophysical methods when assessing, both in field and in laboratory, the parameters depicting the soil state and its stiffness at small strain. With this aim the writer draws the attention to seismic transversal (S) and longitudinal (P) body waves generated both in field, during in-hole tests, and in laboratory using piezocrystals. Within this framework the following issues are discussed:

- Stiffness at very small strain as obtainable from the S and P velocities.
- Difference between fully from near to saturated soils from the measured P-wave velocity.
- Evaluation of undisturbed samples quality based on the comparison of S-waves velocities measured in field and in laboratory respectively.
- Evaluation of porosity and void ratio from measured P and S waves velocity.
- S-wave based evaluation of the coarse grained soils susceptibility to cyclic liquefaction.

Keywords: seismic body waves, stiffness, fully and near to saturated state, porosity, liquefaction.

A Friend's Legacy

"Try to know yourself and your preferences. Listen, observe, investigate: choose your love and love your choice." (Victor de Mello).



And indeed this was Victor de Mello, certainly no ordinary man nor just an engineer.

Both personally and professionally Victor personified excellence, with a deep set of values and an amazing ability to stay connected with those he knew. And I am so proud for being one of his "brothers of blood" as he used to call Harry Poulos, John Burland and myself.

Victor was my mentor and my role-model and has certainly impacted my professional life. I have hugely benefitted from our many inspiring conversations. Occasionally he was a severe critic but his analyses have always

been constructive encouraging my quality work and, however firm in his resolution, always explaining the nature of his disagreement.

It is fascinating to look into Victor De Mello's background, to his philosophical spirit and his working methods. He combined the engineer rigor with a solid passion for life. His interests ranged widely: engineering sciences, geology, philosophy and ethics, flowers, conversation, travel, literature, music, writing, art, women, food, wines and so forth.

He was also a prolific correspondent and Victor's wise thoughts and advices, always unconditionally given on so many occasions, will remain with me.

He used to say "*We professionals beg less rapid novelties, more renewed reviewing of what is already there*" and this is where I want to start from. In this paper I will attempt to continue the lively, sometimes conflictual, channel of communication Victor and I have been carrying on for ages on issues related to the geotechnical site characterization and on the key requisites for a safe and cost-effective design, in which area Victor de Mello made notable contributions.

1. Introduction

Considering the growing importance of the geophysical methods [Stokoe (2011)] for the geotechnical site characterization, this paper focuses on the in-hole techniques, such as cross-hole (CH) and down-hole (DH) tests which, if properly instrumented and performed, can provide reliable values for compression (V_p) and shear (V_s) waves velocity.

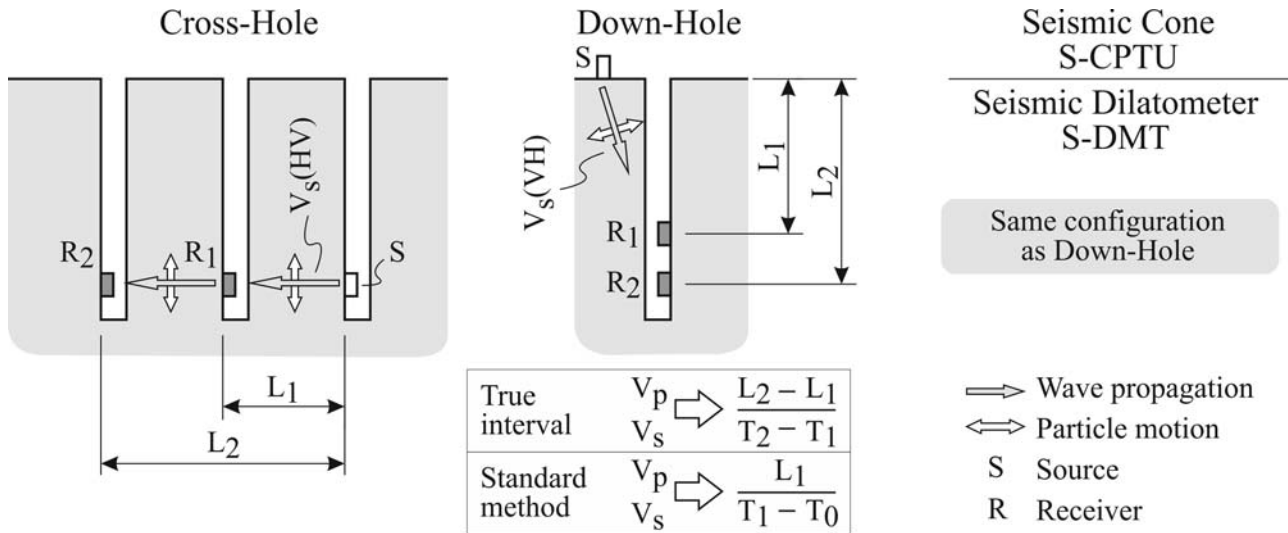


Figure 1 - In-hole geophysical tests.

When it is only requested the knowledge of V_s , reference will also be made to seismic cone penetration tests (S-CPTU) and to seismic Marchetti's dilatometer (S-DMT), equipped to provide a reliable measure of V_s in DH-mode. The main features of CH and DH tests are shown in Fig. 1, while Fig. 2 highlights the seismic waves that can be propagated *in situ*, during CH and DH tests, and in laboratory by means of bender elements (BE).

The generated seismic waves are classified according to the propagation direction (first capital letter) and to the polarization plane (second capital letter).

Figure 2 shows also the soil stiffness at very small shear strain ($10^{-6} \leq \gamma \leq 10^{-5}$), see Rahtje *et al.* (2004) and Cox (2006), that can be computed from the seismic waves velocity, being: G_0 = shear modulus at very small strain, M_0 = constrained modulus at very small strain and ρ_t = bulk soil mass density.

The following aspects, relative to the use of in-hole measured seismic body wave velocities in geotechnical design, are discussed:

1. Stiffness at very small strain: $G_0 = f(V_s)$ and $M_0 = f(V_p)$ (Applicable to V_p propagated through dry soils or at least having $S_r < 90\%$).
2. Distinction between fully saturated and near to saturated soils $\rightarrow f(V_p)$.
3. Assessment of undisturbed samples quality $\rightarrow f[V_s$ (Field) vs. V_s (Lab.)].
4. Evaluation of *in situ* void ratio e_0 by means of Foti *et al.* (2002) approach $f(V_p$ and $V_s)$.
5. Susceptibility of coarse grained saturated soil to cyclic liquefaction $\rightarrow f(V_s)$.

The above topics are only loosely interconnected, thus each subject matter is detailed in a specific section with dedicated closing remarks.

2. Stiffness at Very Small Strain and its Anisotropy

The use of seismic waves velocity allows to evaluate, *in situ* and in laboratory, the shear modulus $G_0 = \rho_t V_s^2$ and the constrained modulus $M_0 = \rho_t V_p^2$.

G_0 is representative of the very initial portion of the soil stress-strain curve (Fig. 3), which, upon loading is linear and in unloading state exhibits a recoverable strain, including a minor amount of the delayed viscous component.

The linear portion of the stress-strain curve is delimited by the linear threshold strain γ_t^l [Lo Presti (1991), Jardine (1992), Ishihara (1996), Hight & Leroueil (2003)].

The γ_t^l for non rocky-like materials usually ranges between 10^{-5} and 10^{-4} , see Fig. 4a which reports also the volumetric threshold shear strain (γ_t^v), see [Dobry *et al.* (1982) and Vucetic (1994)]. The γ_t^v corresponds to the point where a soil element, subject to constant mean effective stress (p^*), under the action of shear stress increase, during

Wave type	Propagation mode	Shape change	Wave velocity	Small-strain modulus
P		Compression 	V_p (V)	$M_0(V)$ $M_0 = \rho_t V_p^2$ $M_0(H)$
			V_p (H)	
S		Distorsion 	V_s (VH)	$G_0(VH)$ $G_0 = \rho_t V_s^2$ $G_0(HH)$
			V_s (HH)	

Wave propagation Particle motion

Figure 2 - Compression (P) and shear (S) waves generated *in situ* and in laboratory tests.

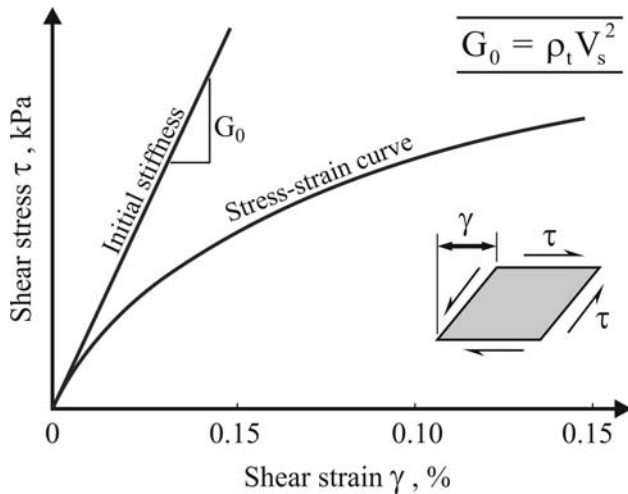


Figure 3 - Small strain shear modulus from seismic tests.

drained loading starts exhibiting plastic strain, whereas, under undrained loading a pore pressure excess is generated.

It can be therefore assumed that G_0 represents the initial tangent shear stiffness of a given geomaterial applicable to both static and dynamic problems, with possibly

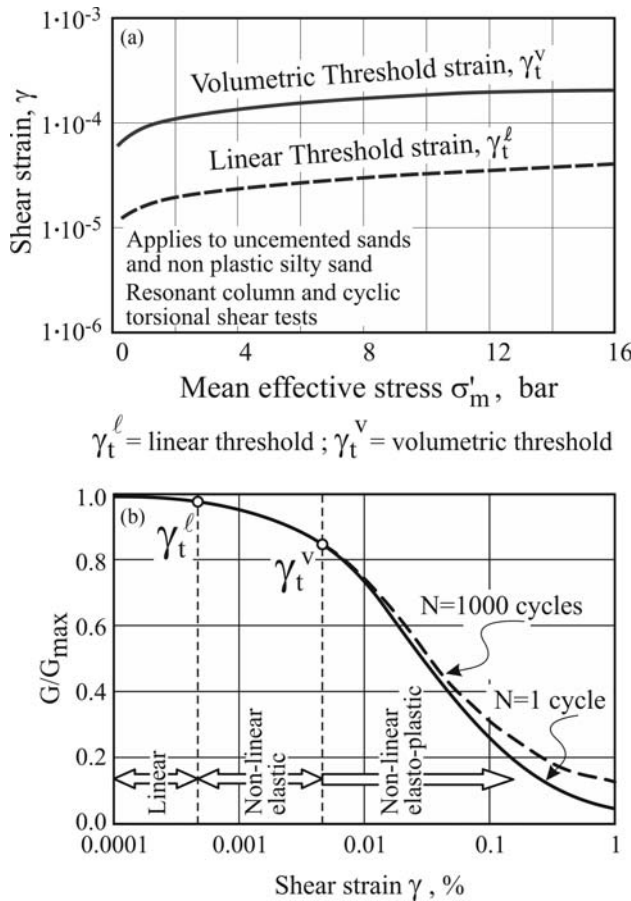


Figure 4 - (a) Small strain shear modulus from seismic tests, Darendelli (1991). (b) Normalized shear modulus degradation curve, Menq (2003).

minor differences due to the strain rate effects involved in two different loadings modes, see Fig. 4b.

This figure, after Menq (2003), reports an example of the normalized shear modulus [$G/G_0 = f(\gamma \geq \gamma_t^l)$] degradation curve as function of the shear strain γ , pointing out the difference between monotonic and cyclic loadings.

As such, G_0 plays a role in the numerical analyses involving complex constitutive soil models, allowing separating elastic from total strains.

Another important function of $G_0(F)$ measured in the field is to allow for the correction of the laboratory determined modulus degradation curve $G(\gamma)$ for disturbance effect. The procedure, see Fig. 5, is based on the available field and laboratory extensive data base, proposed by Ishihara (1996) and makes reference to the following empirical formula:

$$G(\gamma)_{\text{Field}} = C_r \frac{G_0(\text{Field})}{G_0(\text{Lab})} G(\gamma)_{\text{Lab}} \quad (1)$$

being $G_0(F)$ = shear modulus at very small strain ($\gamma \leq \gamma_t^l$) from *in situ* seismic tests, $G_0(L)$ = shear modulus at very small strain ($\gamma \leq \gamma_t^l$) measured in laboratory, $G(L)$ = shear modulus measured in laboratory at the given value of $\gamma \geq \gamma_t^l$, $G(F)$ = corrected field value corresponding to the same value of γ likewise $G(L)$ and C_r = correction factor depending on the sample quality and type.

In his work, Ishihara (1996) provides C_r values as function of the strain level for different kinds of sampling techniques including reconstituted specimens.

In a given soil G_0 and M_0 are controlled by the effective ambient stresses and by the current value of void ratio, reflecting the state of the material.

With reference to the seismic waves propagation and to their computed moduli, the following empirical relations, experimentally validated, [Roesler (1979), Lewis (1990), Lee & Stokoe (1986), Weston (1996)], allow exploring how the current soil state affects V_s , hence G_0 and V_p , thus M_0 respectively:

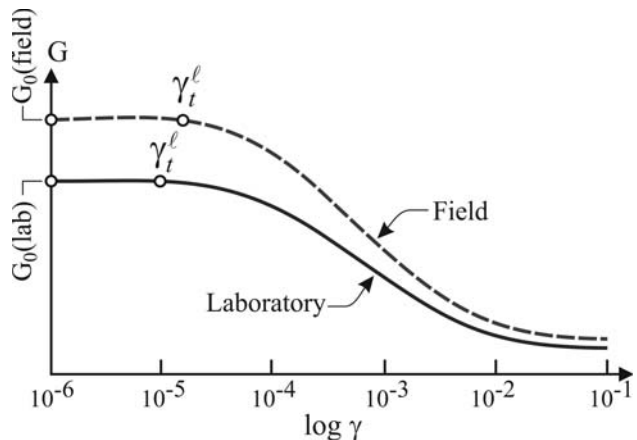


Figure 5 - Ideal field vs. laboratory shear modulus degradation curve, after Ishihara (1996).

$$V_s = C_s [(\sigma'_a)^{na} (\sigma'_b)^{nb} (p_a)^{-(na+nb)}] \sqrt{F(e)} \quad (2.1)$$

$$G_0 = C_G F(e) [(\sigma'_a)^{2na} (\sigma'_b)^{2nb} (p_a)^{-2(na+nb)}] \quad (2.2)$$

$$V_p = C_p [(\sigma'_a)^{na} (\sigma'_b)^{nb} (p_a)^{-(na+nb)}] \sqrt{F(e)} \quad (3.1)$$

$$M_0 = C_M F(e) [(\sigma'_a)^{2na} (\sigma'_b)^{2nb} (p_a)^{-2(na+nb)}] \quad (3.2)$$

being C_s, C_p, C_G, C_M = experimental material constant, na, nb = experimental stress exponent, $F(e)$ = experimental void ratio function, p_a = reference stress = 98.1 kPa, σ'_a = effective stress in the direction of wave propagation and σ'_b = effective stress on polarization plane. Note: In case of $V_s, na \neq nb$, while for $V_p, na = nb$.

The above formulae consent to estimate, for a given soil, the V_s and G_0 as well as the V_p and M_0 values at different stress levels and densities, once the material constants and the void ratio function have been established, see Lee & Stokoe (1986), Lo Presti (1991a), Ishihara (1996), Bellotti *et al.* (1996), Weston (1996), Hoque & Tatsuoka (1998), Fioravante (2000), Kuwano & Jardine (2002).

In the everyday practice, G_0 and M_0 are considered as isotropic elastic body stiffness making simpler also to assess the Young E_0 and bulk B_0 modulus assuming the value of Poisson coefficient of the soil skeleton ν'_0 . With this respect it is worth mentioning that, as confirmed by laboratory tests, ν'_0 at strain level not exceeding the linear threshold, ranges between 0.15 and 0.25, typically exhibiting a trend to decrease with increasing the confining stresses [Hoque (1996), Weston (1996)].

However, the lesson learnt from the propagation of seismic waves *in situ* and in laboratory [Lee & Stokoe (1986), Lee (1993), Bellotti *et al.* (1996), Fioravante (2000), Kuwano & Jardine (2002), Giretti *et al.* (2012)] has demonstrated that in the presence of the level-ground the soil behavior, at very small strain ($\gamma \leq \gamma'_t$), can be better approximated by the cross-anisotropic (= transversally isotropic) linear elastic half-space, with the vertical axis (z) of symmetry and the horizontal plane (xy) of isotropy [Love (1927)]. The relationship, broadly describing the stress-strain behavior of such body, requires determining five independent elastic material constants, see the stiffness matrix in Fig. 6.

For the plane body waves generated on the vertical (xz) or horizontal (yx) planes, White (1965) derived three equations expressing the velocities in terms of five independent material constants of the cross-anisotropic half-space, see Stokoe *et al.* (1991) and Lee (1993).

The difference in velocities of V_p and V_s propagating on xz and xy or yx planes, coinciding with the principal stresses directions respectively, reflect the material *initial anisotropy*.

$$[\sigma'] = [C][\varepsilon]$$

Where $[C]$ = Stiffness matrix (according to Love, 1959)

$$[C] = \begin{bmatrix} C_{11} & C_{12} & C_{13} & 0 & 0 & 0 \\ C_{12} & C_{11} & C_{13} & 0 & 0 & 0 \\ C_{13} & C_{13} & C_{33} & 0 & 0 & 0 \\ 0 & 0 & 0 & C_{44} & 0 & 0 \\ 0 & 0 & 0 & 0 & C_{44} & 0 \\ 0 & 0 & 0 & 0 & 0 & C_{66} \end{bmatrix}$$

- C_{11} = M(H) on the isotropic plane
- C_{33} = M(V) } in plane of the
- C_{44} = G(VH) } symmetry axis
- C_{66} = G(HH) on the isotropic plane
- C_{13} = fifth independent parameter
- C_{12} = M(H) - 2G(HH) dependent parameter

Figure 6 - Stress-strain relationship and stiffness matrix of the cross-anisotropic elastic halfspace, Love (1959).

Dealing with the initial elastic anisotropy ($\gamma \leq \gamma'_t$) of the non rocky-like geomaterials, two components of different phenomenological nature should be distinguished:

- *Fabric* or *structural* anisotropy exhibited by the soil under isotropic state of stress.
- *Stress induced* anisotropy disclosed even by a soil with isotropic fabric when subject to anisotropic stress state.

Referring to the level ground, *i.e.* geostatic stress state, the stress induced anisotropy is governed by the magnitude of earth pressure coefficient at rest K_0 , hence by the soil depositional and post-depositional history.

The initial anisotropy can be quantified in the field measuring, during CH tests, $V_s(HH)$ on the isotropy plane and $V_s(VH)$ along the symmetry axis plane.

The same measurements have been carried out at the copper mine tailings at Zelazny Most (Poland) site yielding initial anisotropy values in terms of $V_s(HH)/V_s(VH)$ ratio ranging between 0.92 and 1.12.

Unfortunately, the five independent constants of the cross-anisotropic geomaterials cannot be determined *in situ*. Four of them: $G_0(HH), G_0(VH), M_0(H)$ and $M_0(V)$ can be assessed from the corresponding shear and compression waves measurable in CH tests.

However, for M_0 values, to ensure that the V_p propagation is entirely controlled by the soil skeleton compressibility, such approach is limited to materials that are either dry or with a satisfactorily low degree of saturation¹.

¹ See also Fig. 8

In these circumstances, the basic studies for cross-anisotropic materials have been mostly carried out in laboratory, testing mainly on reconstituted soil specimens. Three different methodologies have been employed so far:

- Using exclusively the static stress-strain laboratory probing [Hoque (1996), Hoque & Tatsuoka (1998)], however requiring a simplified assumption to assess the fifth independent cross-anisotropy body parameter.
- As above, combining the results of static probing, with the dynamic measurements of seismic waves velocity using bender elements. This methodology has allowed Kuwano & Jardine (2002) to determine all the five independent material constants.
- Using solely seismic waves generated in large calibration chambers [Lee (1985), Lee & Stokoe (1986), Stokoe *et al.* (1991), Bellotti *et al.* (1996), Giretti *et al.* (2012)], as well as in triaxial apparatuses, see Fioravante (2000), all the above five independent material parameters can be determined.

In these tests, usually carried out under biaxial confinement, it can be determined the fifth independent material parameter, even though generating, in the anisotropy plane, the V_p and V_s waves at the angle Θ with respect to the axis of symmetry (z). Lee (1985) and Lee & Stokoe (1986) have pointed out that the propagation of planar waves in xz and zy planes, and not along the principal stress directions, uncouples the *velocity surface* (= the front of the wave normal) from the overlapping *wave surface* (energy ray path). On the other hand, as observed by Stokoe *et al.* 1991 and Lee 1993, for dry silica sands the resulting discrepancy is sufficiently small and leads to minor corrections of the measured ray velocity to obtain the phase velocity.

In the following are given some examples of seismic tests carried out in a large calibration chamber housing specimen 1.2 m in diameter and 1.5 m in height and instrumented with miniature geophones, see Fig. 7. The adopted geophones arrangement allows the generation, under biaxial confinement, of P and S waves in three orthogonal principal stress directions xyz in Fig. 7 as well as of the oblique waves $P(\Theta)$, $S(\Theta)$ inclined at an angle of 45° as regard the axis of symmetry (z), with the oblique shear waves $S(45^\circ)$ polarized in a vertical plane.

Details of the tests experimental setup can be found in Lo Presti & O'Neill (1991) and Bellotti *et al.* (1996). In the second work, it is also illustrated the trial and error computation procedure used to estimate, with the aid of $P(45^\circ V)$ and $S(45^\circ V)$, the fifth independent parameter C_{13} of the stiffness matrix of Fig. 6.

Hereafter are summarized some examples of seismic tests results performed in CC on dry pluvially deposited TS-Ticino river (Bellotti *et al.* 1996) and KS-Calcareous Kenya beach (Giretti *et al.* (2012) sands; the same test sands were employed by Fioravante (2000) to investigate, in a triaxial apparatus, the elastic anisotropy. The test sands characteristic are depicted in Table 1.

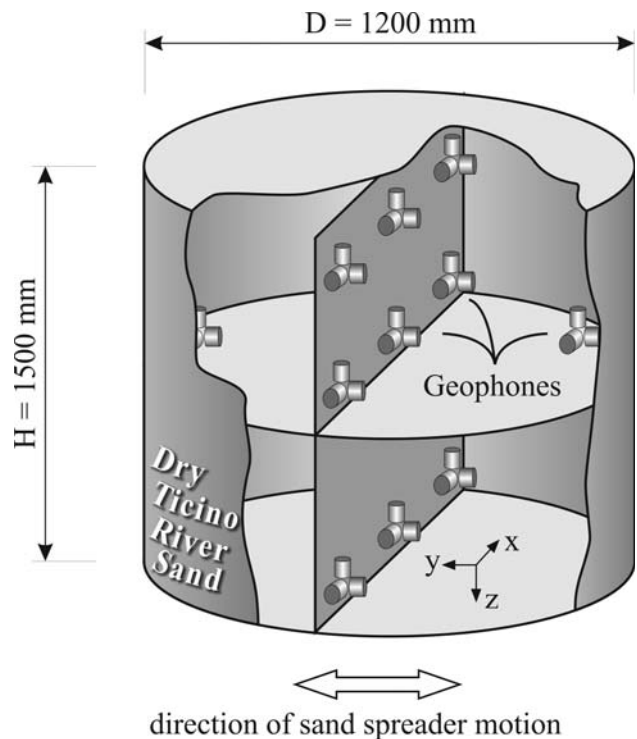


Figure 7 - ISMGEO calibration chamber with geophones to measure the body waves velocity.

Table 1 - Test sands properties.

	Ticino river	Kenya beach
G_s	2.681	2.783
d_{50}	0.55	0.13
C_u	1.69	1.85
e_{min}	0.578	1.282
e_{max}	0.927	1.776
ϕ'_{cv}	33°	40°
	Siliceous	Carbonatic

Tables 2 and 3 show the moduli ratio $G_0(HH)/G_0(VH)$ and $M_0(H)/M_0(V)$ as obtained from CC seismic tests in dry TS and KS.

More details respectively for TS and KS, can be found in the works by Bellotti *et al.* (1996) and Giretti *et al.* (2012).

To sum up, the seismic waves velocity measurement, *in situ* and in laboratory, plays a central role in the evaluation of the soil stiffness at very small strain and of its anisotropy.

The main issues significant to the engineering applications are:

- G_0 corresponding to the initial tangent shear modulus for both static and dynamic loading.
- Knowing G_0 , elastic and plastic strains can be separated.

Table 2 - Dry Ticino river siliceous sand elastic anisotropy.

Medium dense					
	σ'_h/σ'_v	G_{hh}/G_{vh}	M_h/M_v	E_h/E_v	Stress range σ'_v (kPa)
$D_R = 41\%$	0.5	0.96	0.83	0.81	50 to 300
	1.0	1.20	1.20	1.22	50 to 300
	1.5	1.25	1.55	1.52	50 to 300
	2.0	1.44	1.88	1.86	50 to 300
Very dense					
	σ'_h/σ'_v	G_{hh}/G_{vh}	M_h/M_v		Stress range σ'_v (kPa)
$D_R = 88\%$	0.5	1.13	1.05		50 to 300
	1.0	1.15	1.31		50 to 300
	1.5	1.25	1.40		50 to 300

Siliceous river sand, $G_s = 2.681$, $e_{max} = 0.927$, $e_{min} = 0.578$, $C_u = 1.69$, $\phi'_{cv} = 33^\circ$, $F(e) = e^{-1.3}$.

- G_0 inferred from V_s measured in the field offers the possibility to correct the laboratory G vs. γ degradation curves accounting for disturbance effects.
- The generation of $S(HH)$ and $S(VH)$ waves in field and in laboratory consent to estimate the material initial anisotropy.
- Although so far limited to laboratory testing on reconstituted specimens, the generation of seismic waves, alone or in combination with static probing, carried out in the triaxial apparatus consent to study the basic behavior of the elastic cross-anisotropic geomaterials.

3. Fully Saturated vs. Near-To-Saturated Soils

In the last two decades many laboratory and field experiments have proved that the compression wave propagation is an extremely sensitive tool to distinguish fully from

Table 3 - Dry oolitic calcareous Kenya beach sand elastic anisotropy.

Medium dense					
	σ'_h/σ'_v	G_{hh}/g_{vh}	M_h/M_v	E_h/E_v	Stress range σ'_v (kPa)
$D_R = 35\%$	0.5	0.93	0.78	0.79	50 to 500
	1.0	1.12	1.27	1.24	50 to 500
	2.0	1.26	2.05	1.92	25 to 250
Very dense					
	σ'_h/σ'_v	G_{hh}/G_{vh}	M_h/M_v	E_h/E_v	Stress range σ'_v (kPa)
$D_R = 88\%$	0.5	1.09	0.94	0.98	50 to 500
	1.0	1.24	1.27	1.29	50 to 500
	1.5	1.28	2.08	1.93	25 to 250

near to saturated soils: [Ishihara *et al.* (1998); Kokusho (2000); Tsukamoto *et al.* (2001); Ishihara *et al.* (2004); Nakazawa *et al.* (2004); Ishihara *et al.* (2004), Valle Molina (2006)]. The compression wave propagation can be used both in the field via in-hole geophysical methods and in the triaxial cell instrumented by means of BE tests, *e.g.*: Fioravante (2000); Tsukamoto *et al.* (2001); Kuwano & Jardine (2002); Valle Molina (2006), Valle Molina & Stokoe (2012).

Figures 8 and 9 show the results of laboratory experiments aimed at exploring the dependence of V_p on the saturation degree. The results confirm the extreme sensitivity of the P -wave velocity to even small deviations from the full saturation, occurring when V_p exceeds 1450 to 1500 m/s, and correspond to the compression wave in water velocity.

Figure 10 presents the result of CH tests carried out from the sea bottom of the Venice Lagoon as part of the site characterization for the Mose barriers project [Jamiolkowski *et al.* (2009)] aimed at safeguarding this unique city

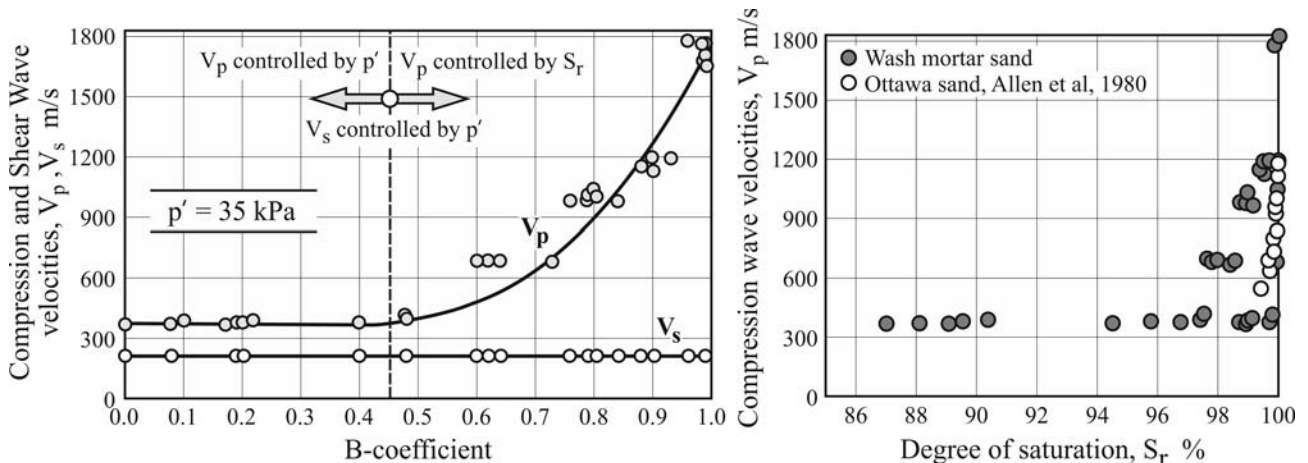
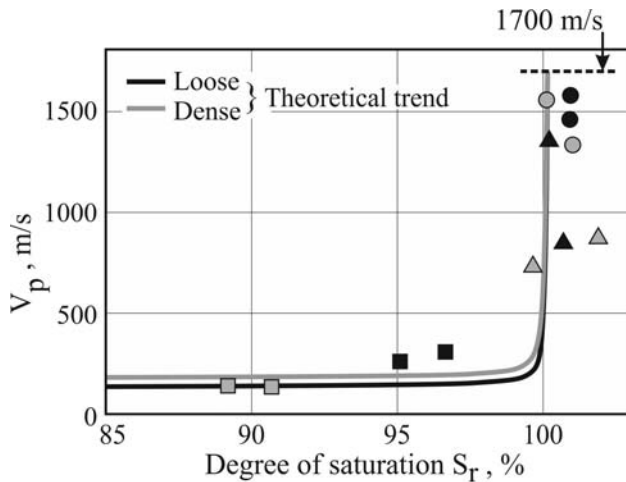


Figure 8 - P-waves and S-waves dependence on saturation degree, Valle-Molina (2006).



	D _R %	Saturation method	S _r %
■	90.2-93.5	Atmosphere	89.2-90.7
□	15.3-25.9	Atmosphere	95.1-96.7
▲	96.7-97.7	Vacuum	100
△	25.4-29.9	Vacuum	100
●	96.2-99.7	Vacuum+CO ₂	100
○	24.6-31.2	Vacuum+CO ₂	100

Figure 9 - Compression wave velocity vs. saturation degree, Takahashi *et al.* (2001).

from high tides. This figure shows $V_p(H)$ as well as $V_s(HV)$ and $V_s(HH)$ resulting from CH tests, together with the relevant lagoon soil profile.

The V_p profile highlights the presence, below the sea bottom, of an unsaturated soil zone, ≈ 12 m thick, due to marsh gas.

The capacity of V_p to detect the presence in the subsoil of near to saturated spots, plays a crucial role in evaluating the susceptibility of coarse grained soils to cyclic and monotonic liquefaction during undrained loading [Ishihara *et al.* (1998); Grozic *et al.* (1999, 2000); Ishihara *et al.* (2004), Lee *et al.* (2005)]. Figure 11 displays the cyclic resistance ratio (CRR) obtained from undrained triaxial tests of the near to saturated Toyoura sand, normalized with respect to the CRR of the same sand at full saturation, see Ishihara *et al.* (1998) and Tsukamoto *et al.* (2001).

The V_p capability to map the saturation surface position in the subsoil, finds many important applications in the engineered constructions experiencing complex hydraulic regime, variable in time and space.

A typical example is the second world largest copper tailings storage disposal, whose peculiar features can be inferred from Fig. 12. At this Polish site, in Zelazny Most, since 1993 CH tests are being carried out periodically on the pond beaches, to map the position of the saturation line in the tailings, [Jamiolkowski *et al.* (2010)]. Figure 13 shows the location of 9 CH tests performed during the 2011 campaign.

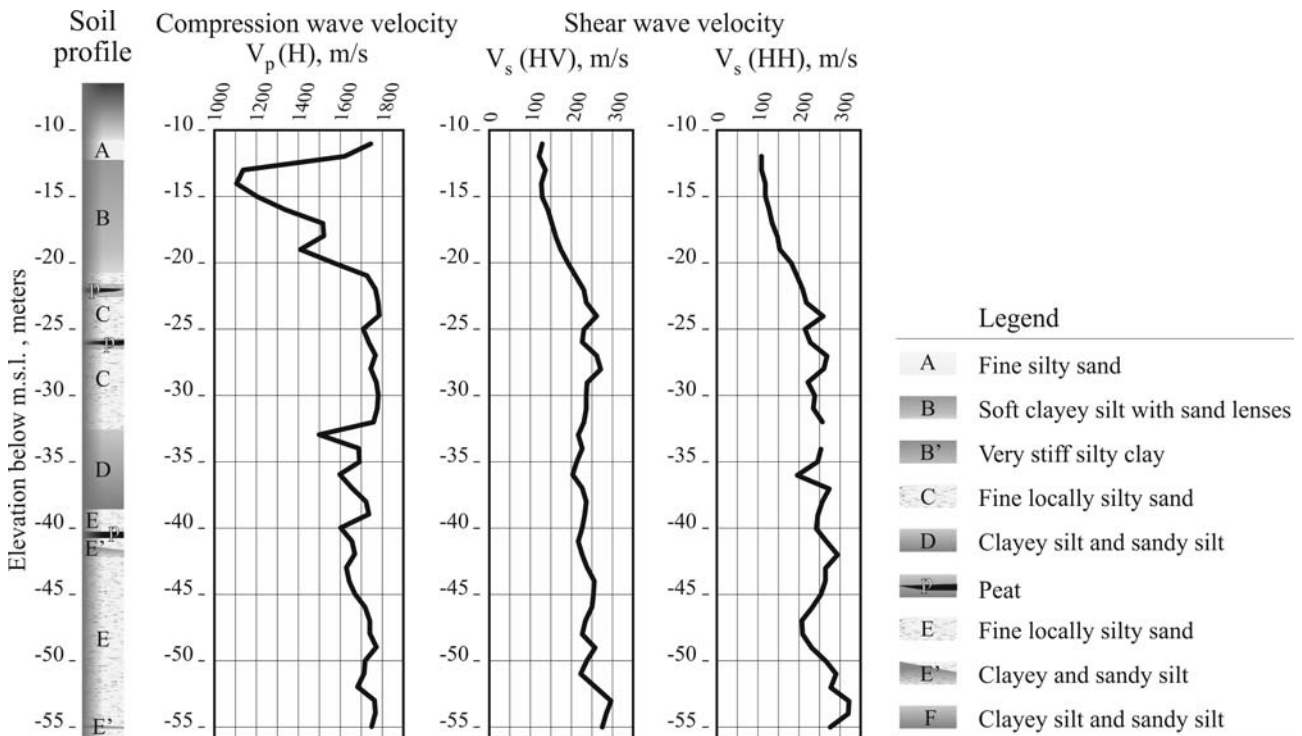


Figure 10 - Venice Lagoon, Chioggia inlet- Cross-hole test results.

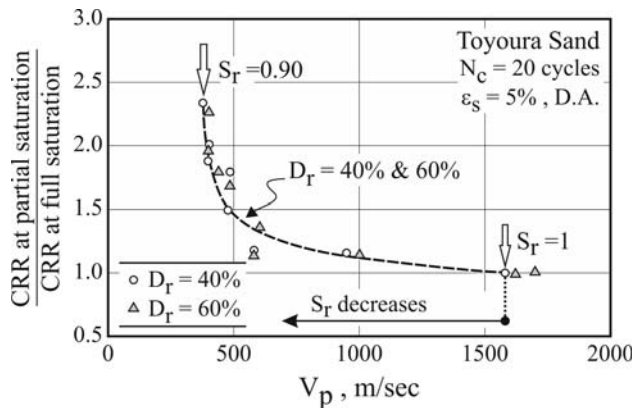


Figure 11 - Cyclic resistance ratio dependence on saturation degree Ishihara *et al.* (1998), Tsukamoto *et al.* (2001).



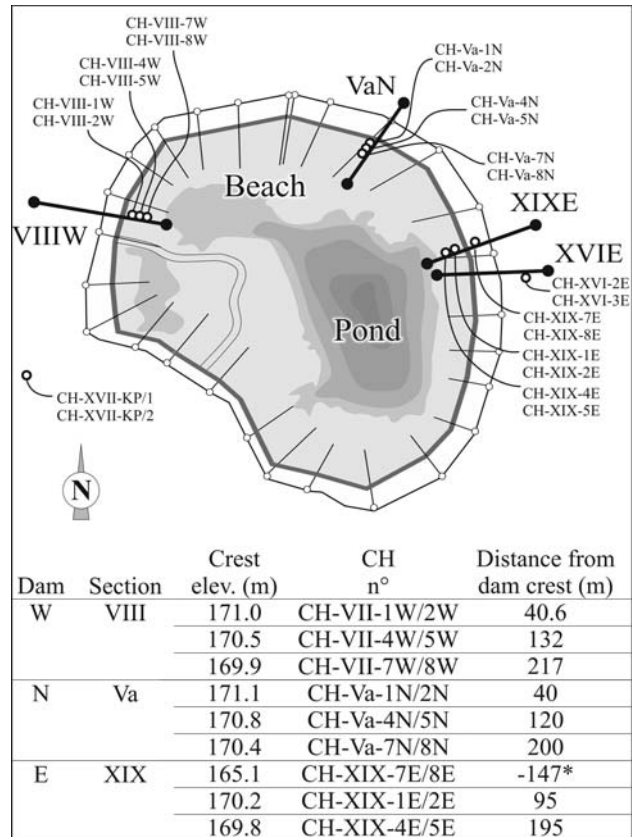
Maximum dam height: 61 m
 Total volume stored: $506 \times 10^6 \text{ m}^3$
 Storage rate: $\cong 17.5 \times 10^6 \text{ m}^3/\text{annum}$
 Area covered: 14.2 km^2
 Dam's perimeter: 14.5 km
 Operation time: 1977 throughout 2042

Figure 12 - Zelazny Most (Poland), copper tailings disposal: aerial view.

Figures 14 through 16 display the depth position of the saturation line in the tailings, as determined based on the V_p measured in CH tests at variable distance from dam crest for cross-sections in correspondence of the West, North and East dams respectively. As the figures show, the measured V_p value, allows recognizing the presence of saturated tailings at a depth below which V_p remains greater than 1450 to 1500 m/s. Moreover, the profiles of V_p vs. depth show also the presence, in the tailings, of the perched water horizons. See Figs. 15 and 16 where the perched water horizons are labeled with the symbol P_H .

From the above one can deduce that:

- The measured V_p is an extremely sensitive tool to distinguish *in situ* and in laboratory fully ($S_r \cong 100\%$) from near to saturated ($90\% \leq S_r < 100\%$) state; see Fig. 9 after Tsukamoto *et al.* (2001) and the recent work by Valle Molina & Stokoe (2012).



(*) Beyond the first dam crest.

Figure 13 - Zelazny Most: Cross-hole tests location.

- This V_p feature represents a simple and reliable tool to map the distribution of fully and nearly to saturated soil deposits *in situ*.
- In the last decade there have been many attempts to correlate Skempton's (1954) pore pressure coefficient B measured in laboratory against the velocity of the compression wave, [Kokusho (2000), Tsukamoto *et al.* (2001), Takahashi *et al.* (2006), Valle Molina & Stokoe (2012)].

4. Quality Assessment of Undisturbed Samples

In case of homogeneous low permeability clays, quality undisturbed samples can be evaluated in laboratory measuring the sample suction p , immediately after its retrieval from the ground, [Skempton (1961), Chandler *et al.* (2011)]. This approach is quite complex, see Chandler *et al.* (2011) and time consuming thus not routinely employed. Moreover, it is restricted to homogeneous fine grained soils able to preserve high suction after zeroing of the total *in situ* stress as results of sample retrieval.

This prompts to develop some easier semi-empirical criteria to assess undisturbed samples quality.

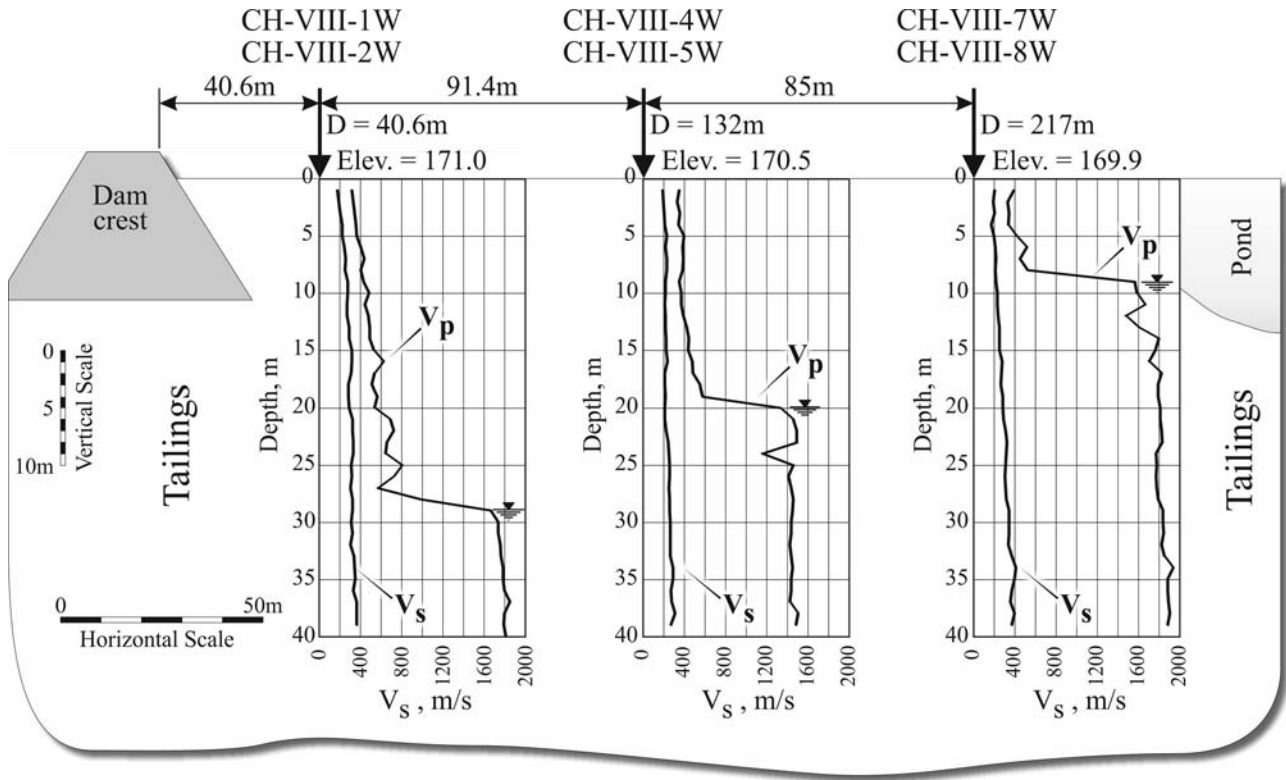


Figure 14 - West dam, cross-hole tests results

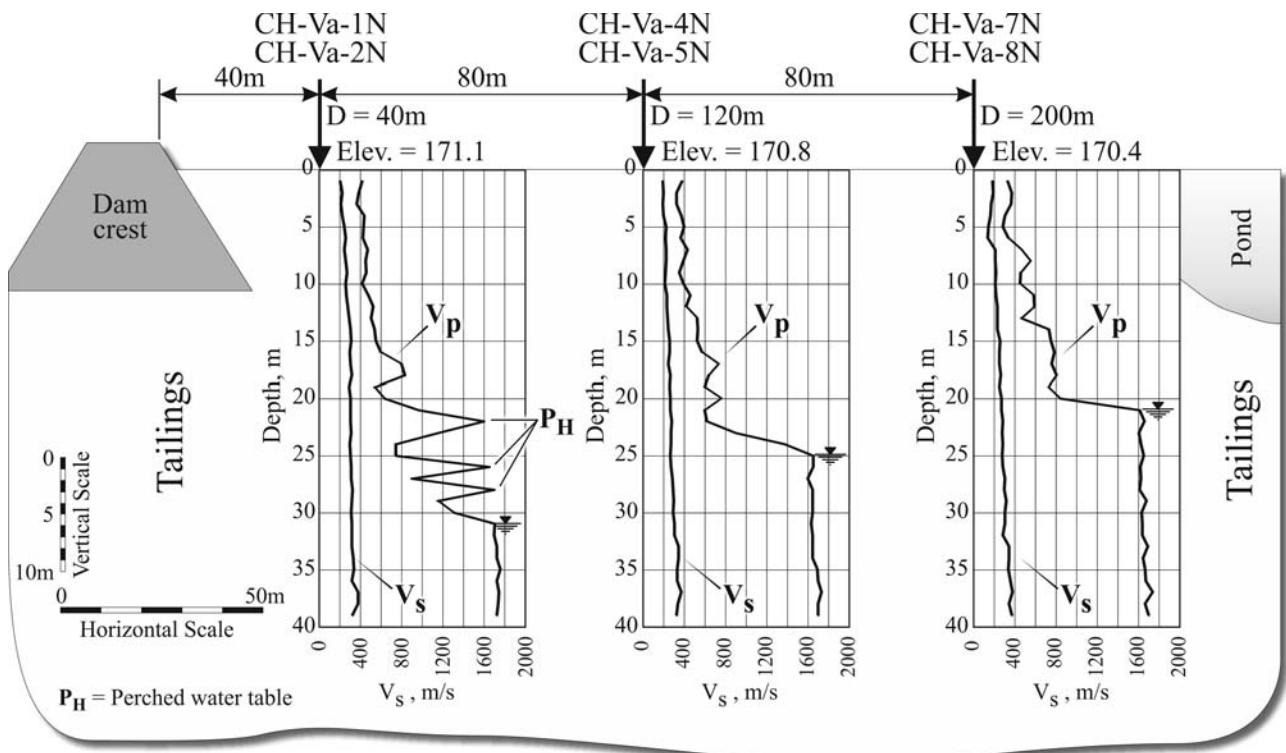


Figure 15 - North dam, cross-hole tests results.

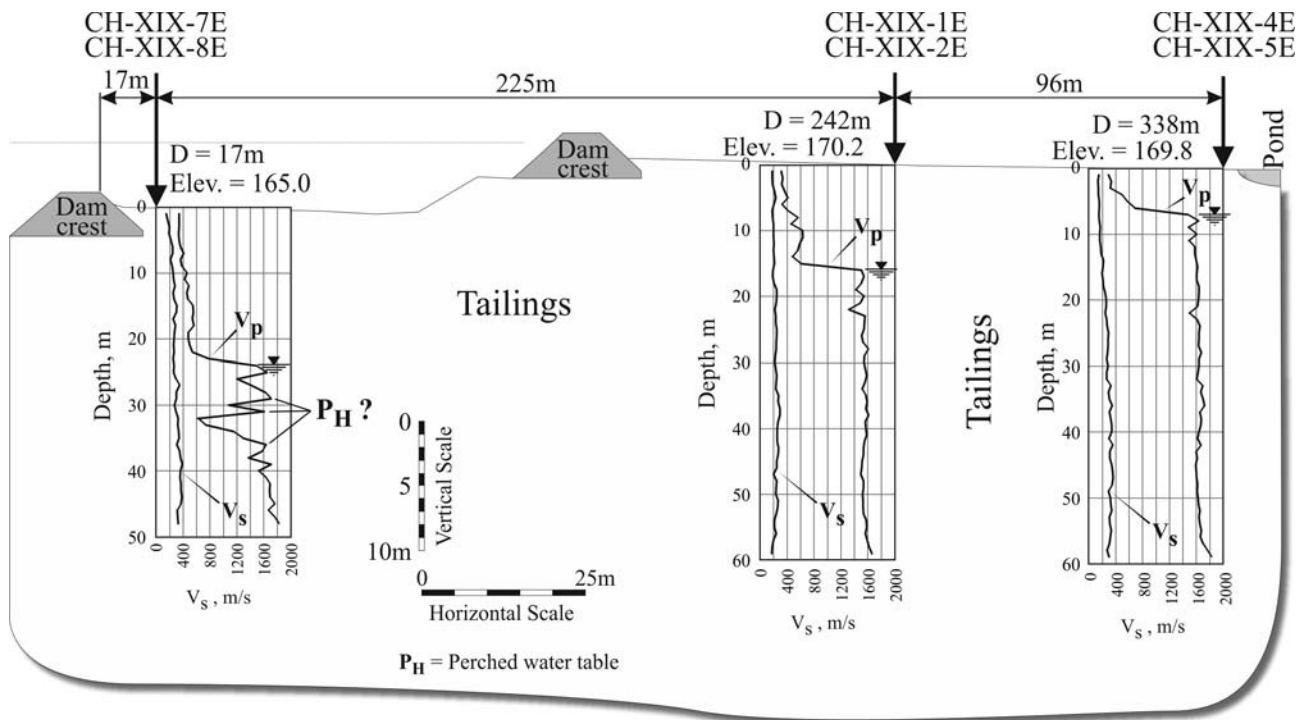


Figure 16 - East dam, cross-hole tests results.

With this respect, a widely used criterion has been proposed by Lunne *et al.* (1997; 2006) for fine grained soils in terms of $\Delta e/e_0$ ratio, being:

- Δe = reduction of the void ratio during one dimensional recompression of undisturbed specimen to *in situ* vertical effective stress σ'_{v0} existing at a depth from which the sample were retrieved.
- e_0 = *in situ* void ratio.

The other criterion, applicable to both coarse and fine grained soils [Sasitharan *et al.* (1994); Landon *et al.* (2007) De Groot *et al.* (2011); Fioravante *et al.* 2012)] is based on the comparison of normalized shear wave velocity $V_{s1}(L)$ measured on laboratory specimens with that measured in the field $V_{s1}(F)$ by means of one of the methods recalled in Fig. 1.

The values of $V_{s1}(F)$ and $V_{s1}(L)$ are computed by means of the formula 4, a somehow simplified version than Eq. 2.1, considering that the separate values of exponents na and nb are difficult to measure and therefore rarely available:

$$V_{s1}(L) = V_s \left(\frac{2p_a}{\sigma'_{v0} + \sigma'_{h0}} \right) \quad (4)$$

where $V_s(F)$ = shear wave velocity measured in the field at the same depth the sample has been retrieved, $V_s(L)$ = shear wave velocity measured in laboratory on the specimen reconsolidated to the best estimate of the *in situ* geostatic stresses at the same depth the sample has been

retrieved, p_a = reference stress = 98.1 kPa, σ'_a = effective stress in the wave propagation direction, σ'_b = effective stress on the plane of the wave polarization, ns = stress exponent $na+nb$, pertinent to $V_{s1}(F)$, σ'_{v0} = effective vertical stress at the sampling depth, σ'_{h0} = effective horizontal stress at the sampling depth, ns = stress exponent $na+nb$, pertinent to $V_{s1}(L)$.

The closer $V_{s1}(L)/V_{s1}(F)$ ratio is to unity, the better the quality of undisturbed sample.

This ratio can also be used to estimate the mechanical characteristics of the specimens reconstituted in laboratory that the soil, in undisturbed state, should have *in situ*.

Overall, exponents np and ns , the former pertinent to V_p , vary within a relatively narrow range (0.22 to 0.25) in case of fine grained soils and uniform sands but tend to increase in coarse gravelly sand and sandy gravel as the uniformity C_u coefficient increases [Weston (1996)], see Fig. 17. This figure adapted after the quoted work by Weston, with the support of some writer's data, gives the stress exponents n_s and n_g from V_s and G_0 respectively determined experimentally in laboratory tests on the reconstituted specimens.

The quality evaluation of three examples based on $V_{s1}(L)/V_{s1}(F)$ ratio is hereafter presented.

The *first* example deals with undisturbed samples of sandy gravel 600 mm in height (H_s) and 300 mm in diameter (D_s) retrieved on the Sicilian shore of Messina Strait by means of the freezing technique [Fioravante *et al.* (2012)], see Fig. 18.

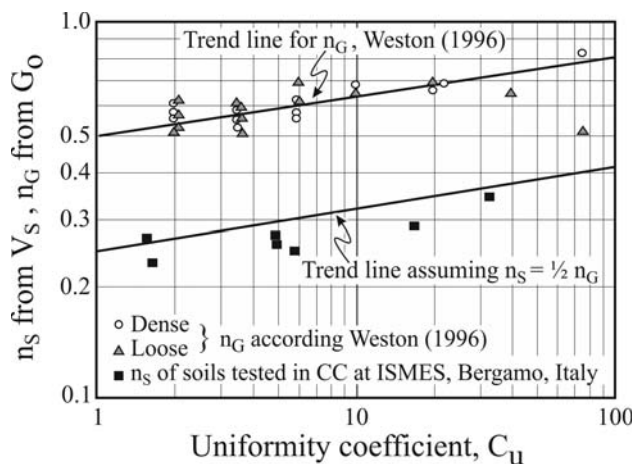


Figure 17 - Stress exponent n_s from V_s and n_G from G_0 , adapted after Weston (1996).

Figure 19 shows the comparison between $V_{s1}(F)$ measured during CH test and $V_{s1}(L)$ obtained from bender element (BE) tests.

Due to the large dimensions of the gravelly particles ($63 \leq d_{max} \leq 100$ mm; $3 \leq d_{50} \leq 16$ mm; $10 \leq C_u \leq 35$), to measure the reliable values of V_s the propagation seismic waves through laboratory specimens, need to fulfill the ASTM D 2845 (1997a) requirements, see also: Sanchez-Salinero *et al.* (1986), Viggiani & Atkinson (1995), Brignoli *et al.* (1996), Jovicic *et al.* (1996), Pennington (2001), Arroyo & Greening (2002) and Maqbool *et al.* (2004).

In the examined case, the characteristics of the generated shear waves during BE tests were as follows:

- Wave mean length: $\lambda_m = 25$ mm; applied frequency: $f = 10$ kHz; $H_s/D_s = 2.0$; $D_s/\lambda_m = 12.0$; $\lambda_m/d_{50} = 2.5$; $H_s/\lambda_m = 24.0$.
- The above values fulfill the ASTM recommendations, with the exception of λ_m/d_{50} ratio which should be ≥ 3.0 .

The *second* example refers to undisturbed samples of fine to medium sand retrieved by means of freezing, see Fig. 20 at the Tyrrhenian shore close to Gioia Tauro, in Southern Italy.

Table 4 reports the values of $V_{s1}(L)/V_{s1}(F)$ ratio as obtained for the tested undisturbed samples. Again in this case, $V_s(L)$ has been measured by means of BE tests while $V_{s1}(F)$ was obtained from CH test whose results².

The resulting values of V_{s1} -ratio, probably except for the one from a 24.5 m depth, confirm the tested samples high quality.

The *third* example deals with the undisturbed sampling of very uniform stiff to hard OC clay, see Fig. 21, retrieved at the Porto Empedocle site on the Eastern Sicilian Coast. In this case, besides using the available V_{s1} ratio, the quality of undisturbed samples has been evaluated from suction measured by means of Ridley & Burland (1993) transducer, carried out soon after the samples retrieval, see Chandler *et al.* (2010) and also referring to the Lunne *et al.* (1997, 2007) criterion based on the ratio of $\Delta e/e_0$ measured in oedometer tests.

Table 5 shows the comparison for a number of Porto Empedocle clay samples between $V_{s1}(L)/V_{s1}(F)$ and $\Delta e/e_0$ ratios together with the ratio of p_s/p'_0 , being: p_s = measured suction in the sample, p'_0 = the best estimate for mean *in situ* effective stress at the sampling depth. In the case in hand, all the three used approaches indicate the excellent quality of tested samples.

The information collected by De Groot *et al.* (2011) supports the idea that both ratios, $V_{s1}(L)/V_{s1}(F)$ and $\Delta e/e_0$, as shown in Fig. 22 are useful and complementary tools when evaluating undisturbed samples quality.

Basically, based on the above the following comments apply:

- $V_{s1}(F)$ reflects *in situ* soil state, fabric, aging and particles bonding.
- $V_{s1}(L)$ has to be assessed on specimens reconsolidated to the best estimate of *in situ* geostatic stresses.

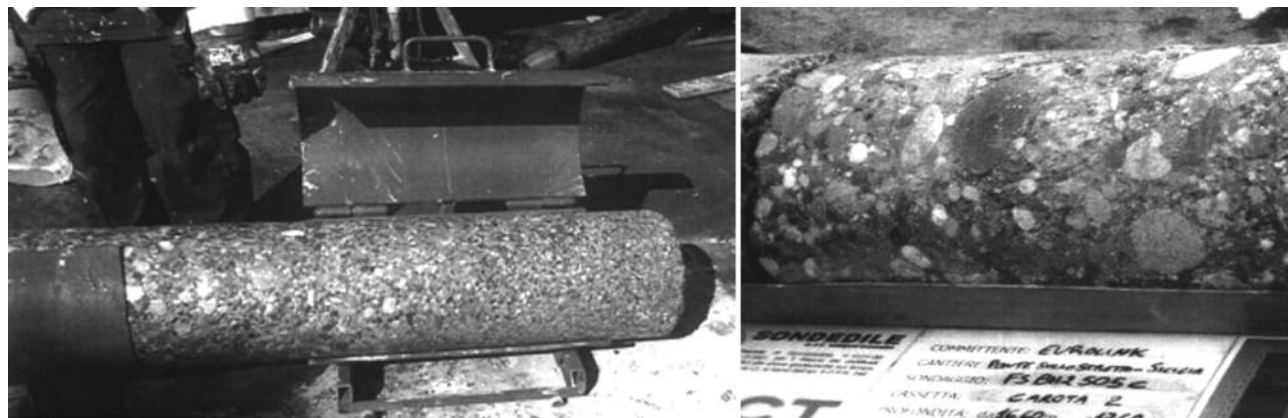


Figure 18 - Messina Strait sandy gravel, undisturbed sample.

² See Fig. 25.

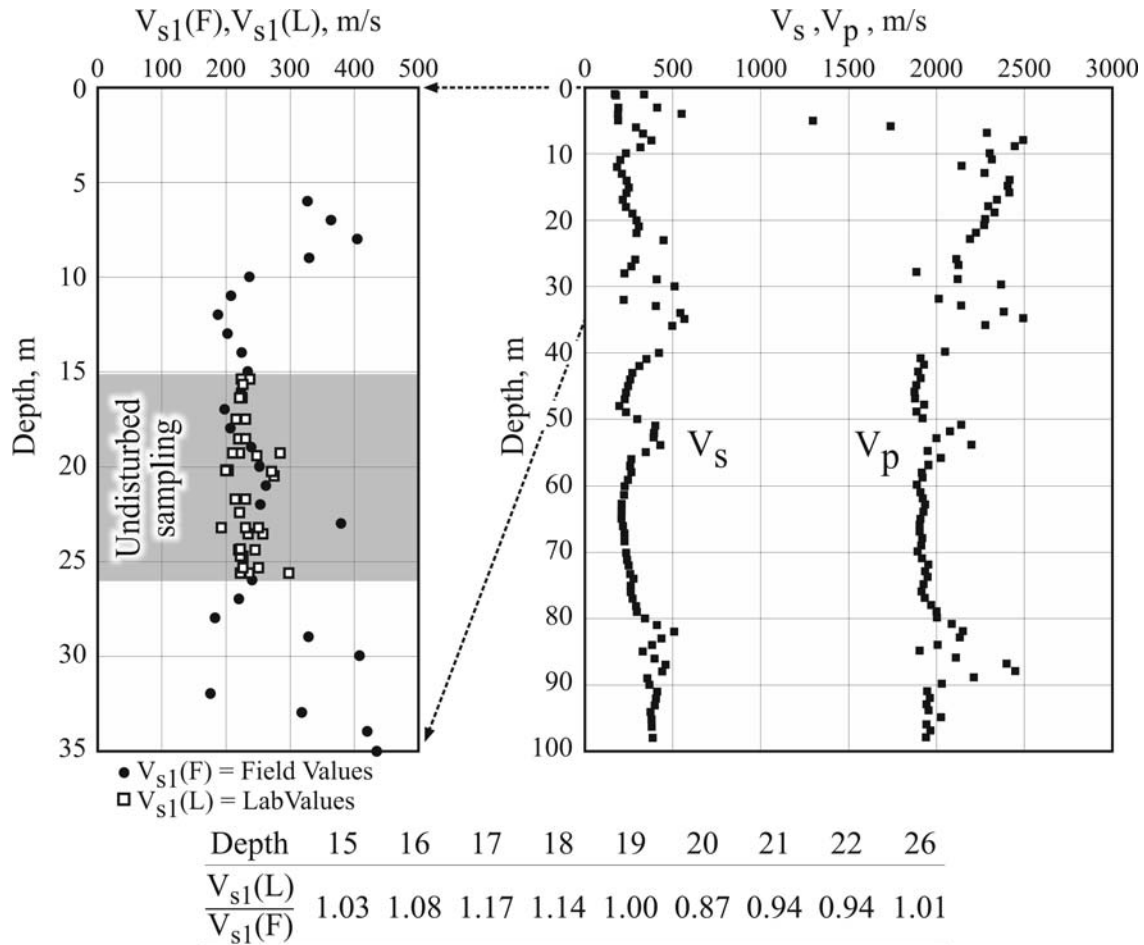


Figure 19 - Messina Strait- $V_{s1}(F)$ from cross-hole test vs. $V_{s1}(L)$ from bender element tests.



Figure 20 - Gioia Tauro, fine to medium sand, undisturbed sample.

- The main uncertainty in determining $V_{s1}(L)$ is linked to an appropriate selection of the laboratory horizontal consolidation stress.
- The closer $V_{s1}(L)/V_{s1}(F)$ is to one, the better the quality of the specimen tested in laboratory.
- Unlike other methods for the assessment of undisturbed samples quality (e.g. suction measurements or the comparison of the void ratio reduction after the specimen 1-D

Table 4 - Gioia Tauro- $V_{s1}(F)$ from cross-hole test vs. $V_{s1}(L)$ from bender element tests.

Depth (m)	$V_{s1}(F)$ (m/s)	$V_{s1}(L)^*$ (m/s)	$V_{s1}(L)/V_{s1}(F)$
24.5	315	227	0.72
28.6	274	222	0.81
30.2	245	230	0.94
31.0	265	227	0.87

(*)BE tests on undisturbed samples obtained by *in situ* freezing.

Table 5 - Porto Empedocle OC clay – Multiple approach to sample quality assessment.

Depth (m)	$\Delta e/e_0$	$V_{s1}(L)/V_{s1}(F)$	p'_s/p'_o
28.6	0.0093	0.984	0.983
31.3	0.0069	0.983	1.078
31.2	0.0059	0.973	1.082
49.8	0.0112	0.984	0.852
53.1	0.0032	0.972	0.938
56.1	0.0052	0.992	0.991



Figure 21 - Porto Empedocle, very stiff to hard clay, undisturbed sample.

recompression to the *in situ* effective overburden stresses), the $V_{s1}(L)/V_{s1}(F)$ ratio can be used in both fine and coarse grained geomaterials.

5. Evaluation of *In Situ* Void Ratio

The geomaterials *in situ* porosity n_0 and void ratio e_0 are important state parameters, crucial for a thorough site characterization when working out many geotechnical boundary value problems.

The assessment of n_0 or e_0 , while routinely determined via laboratory tests on undisturbed samples of fine grained soils, results by far more complex and expensive when dealing with coarse grained soils in which undisturbed sampling [(Yoshimi *et al.* (1978), Hofmann (1997), Yoshimi (2000), Huang *et al.* (2008))] is still far to become a common practice.

To overcome this restraint, several empirical correlations have been proposed based on various penetration tests [Schmertmann (1978), Skempton (1986), Cubrinovski & Ishihara (1999), Jamiolkowski *et al.* (2001)] and *in situ* relative density (D_r), which, in combination with laboratory determined maximum (e_{max}) and minimum (e_{min}) void ratio allow estimating, in first approximation, the e_0 .

In this circumstance, the researchers and practitioners attention was drawn by Foti *et al.* (2002) work who, within the frame of Biot (1956) linear theory of poroelasticity, has developed a procedure to compute *in situ* e_0 or n_0 via inversion of the seismic waves V_p and V_s measured in the in-hole geophysical tests.

The formula by Foti *et al.* (2002), applicable to *fully saturated* soils only is reported here below:

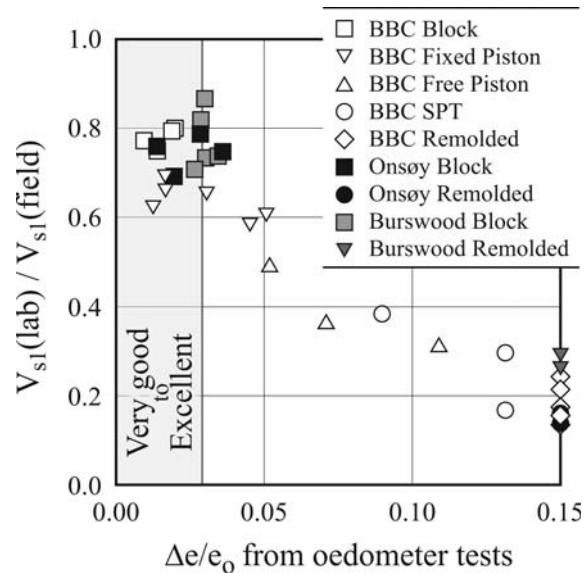


Figure 22 - Undisturbed clay sample quality assessment-Field vs. laboratory criterion, DeGroot *et al.* (2011).

$$n = \frac{\rho_s \left[\rho_s^2 - \frac{4(\rho_s - \rho_f)B_f}{V_p^2 - 2\left(\frac{1-\nu_s}{1-2\nu_s}\right)V_s^2} \right]}{2(\rho_s - \rho_f)} \quad (5)$$

where ρ_s = soil particles mass density, ρ_f = pore fluid mass density, B_f = bulk modulus of pore fluid, ν_s = Poisson ratio of soil skeleton.

Since its publication this formula has been calibrated against laboratory tests results carried out on good quality undisturbed samples of fine grained geomaterials [Foti & Lancellotta (2004), Arroyo *et al.* (2007), (Jamiolkowski *et al.* (2009)), yielding, overall, satisfactory results.

In the following are compared, and when appropriate commented, three examples of void ratio e_0 computed from seismic waves velocity measured in CH tests and those obtained in laboratory on high quality undisturbed samples.

The *first* examples, see Fig. 23, compares n_0 values measured in laboratory on high quality undisturbed samples of soft lightly OC Pisa clay with those computed from V_p and V_s .

The *second* example in Fig. 24, compares the e_0 measured in laboratory on the undisturbed samples of sandy gravel retrieved by means of freezing, at Messina Strait and those computed from the V_p and V_s measured in the CH test located nearby the in-hole from which the frozen samples have been retrieved. The e_0 computed values on average result to be 10 to 15 percent lower than those determined in laboratory (Fioravante *et al.* 2012). The reasons for this difference can be attributed to a combination of the following factors: uncertainties involved in the accuracy of measured

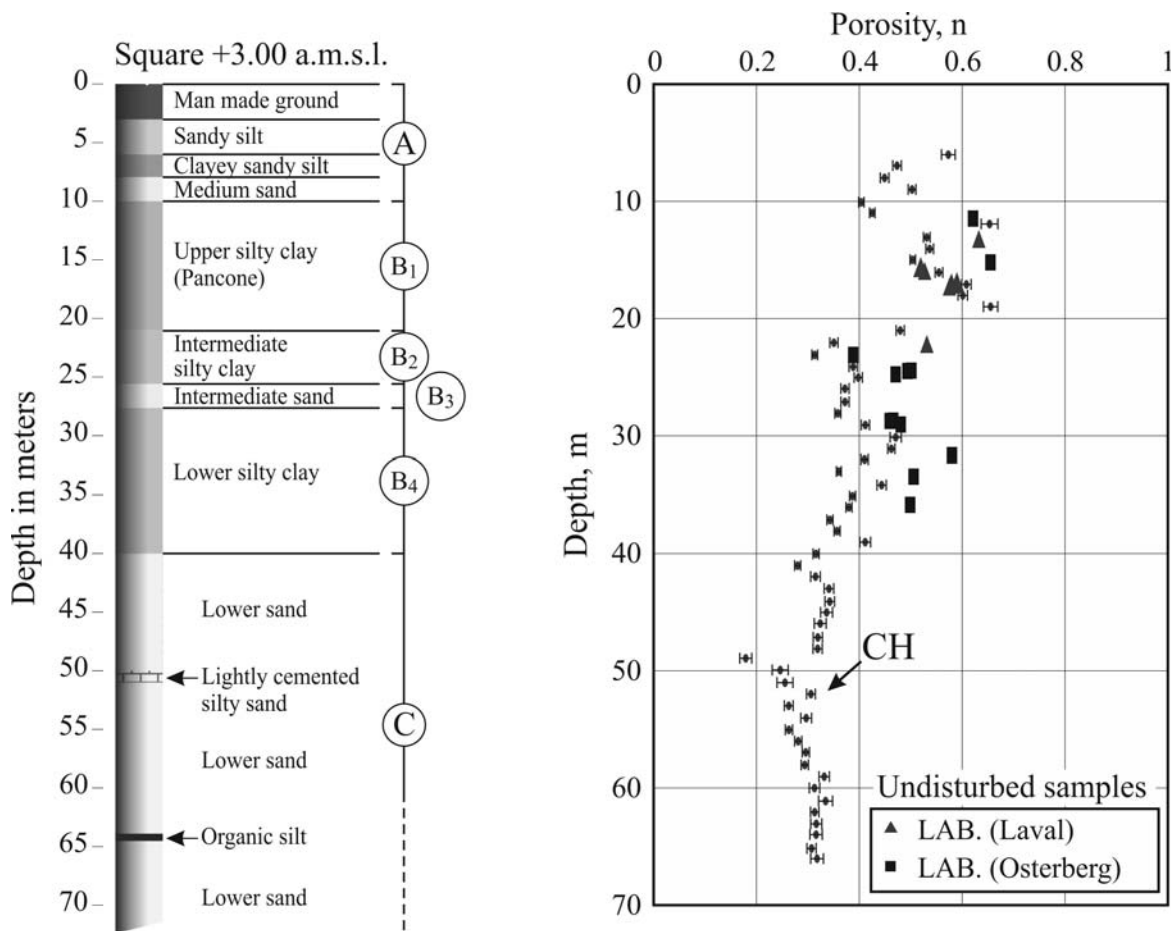


Figure 23 - Pisa clay- Porosity from V_p and V_s vs. laboratory determined values.

V_p and V_s ; the large disparity between the volume of the undisturbed specimen tested in laboratory and the volume of soils involved in waves propagation during CH testing associated with the spatial variability of the sandy gravel deposit in question.

The *third* examples in Fig. 25, displays the comparison between e_0 measured in laboratory on undisturbed frozen samples of fine to medium sand retrieved at Gioia Tauro site, with those computed from the V_p and V_s measured in the CH test located in the vicinity of the sampling in-hole. In this case, the agreement between e_0 values measured and computed is satisfactory.

However, as to the reliability of the *in situ* void ratio, as computed from V_p and V_s measured in the state of the art CH tests, not all the experimental evidences, collected so far by the writer, have yielded satisfactory comparisons with the laboratory determined e_0 . Figure 26 reports the extreme case of a very stiff to hard homogeneous marine Pliocene clay at Porto Empedocle site where the e_0 computed from V_p and V_s significantly underestimates the laboratory measured values by almost a constant offset of about 30 to 50 percent of the laboratory values.

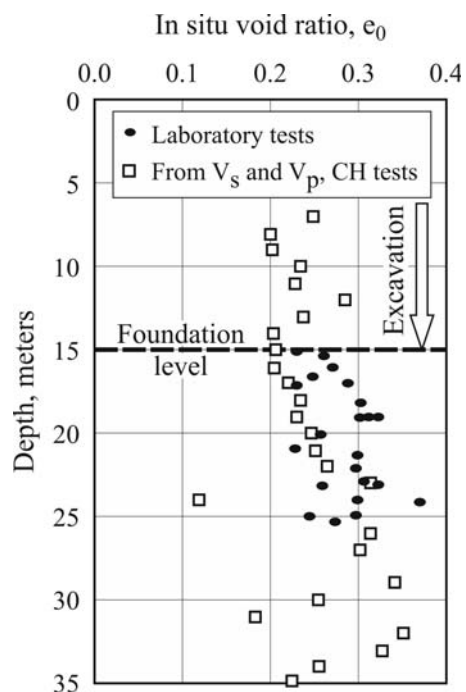


Figure 24 - Messina Strait – Void ratio from V_p and V_s vs. laboratory determined values.

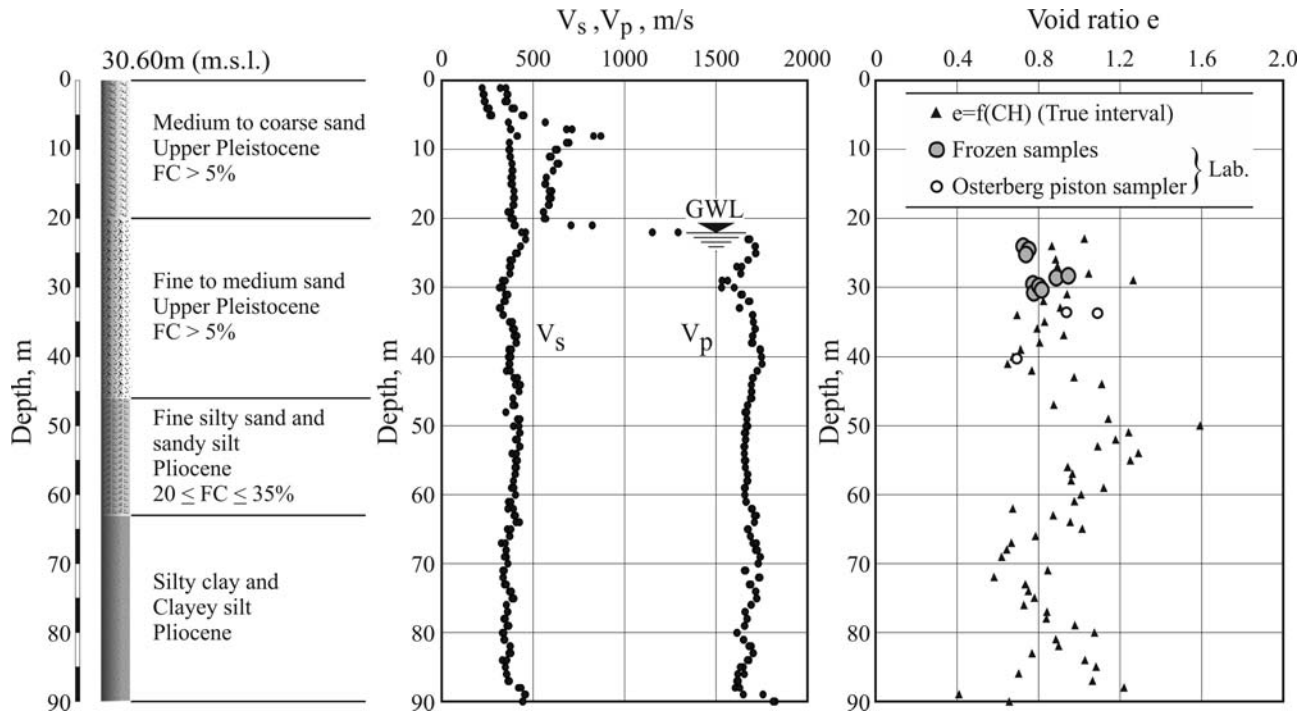


Figure 25 - Gioia Tauro – Void ratio from V_p and V_s vs. laboratory determined values.

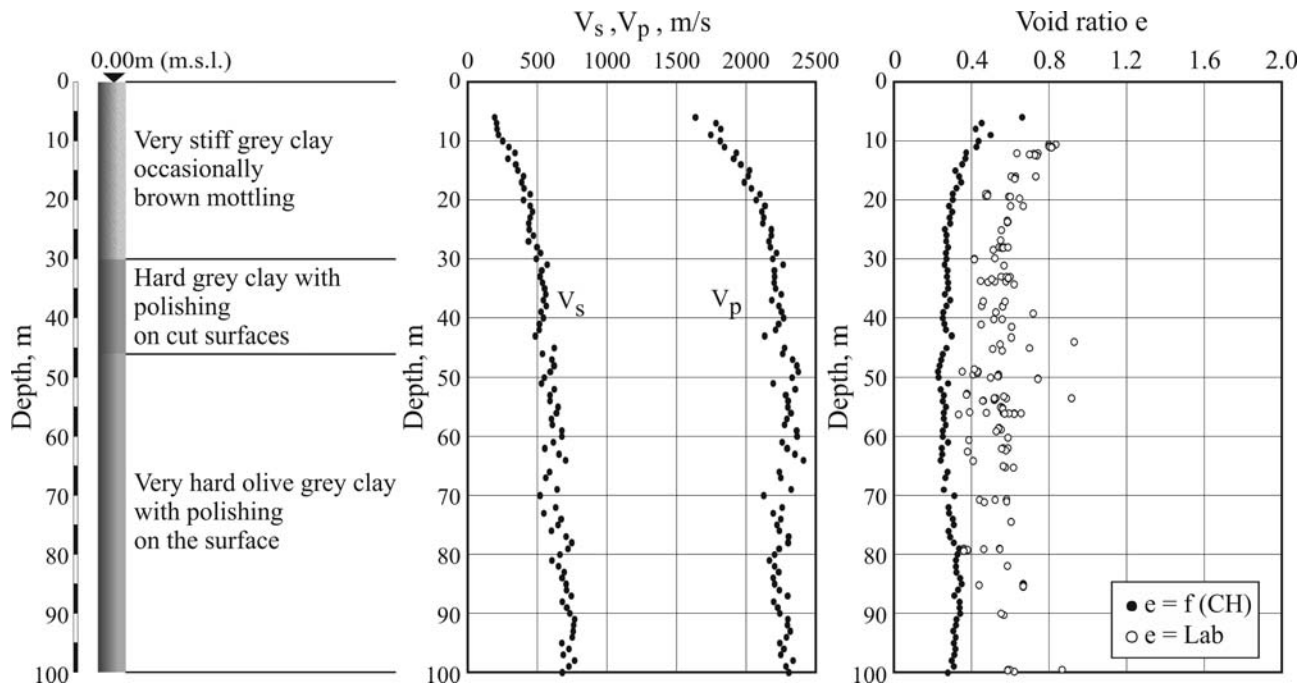


Figure 26 - Porto Empedocle – Void ratio from V_p and V_s vs. laboratory determined values.

A few similar examples have raised the issue of the accuracy and reliability of *in situ* void ratio computed from V_p and V_s . This subject has been addressed by Foti (2003) who has investigated the error propagation of the measured seismic waves velocities in the porosity computed by means of Foti *et al.* (2002) formula.

As it can be expected, dealing with an inverse problem, the reliability of the computed e_0 or n_0 is very sensitive to the accuracy of the measured key input parameters, V_p and, to a less extent, V_s .

Figure 27 exemplifies how, on the measured seismic waves velocity, in the range of V_p and V_s characteristic for

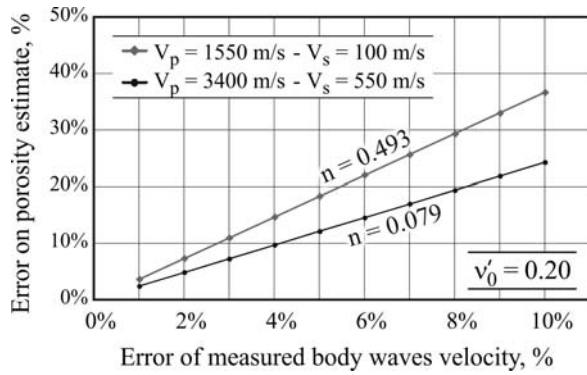


Figure 27 - Error propagation in computing porosity from V_p and V_s as per Foti (2003).

non rock like geomaterials, the error affects the computed porosity. It can be observed that within the range of the considered V_p and V_s , the error on the measured seismic wave velocity amplifies, by three times that of the computed porosity.

Moreover, Lai & Crempien (2012), investigating the stability of the inversion procedure to compute the porosity after the formula by Foti *et al.* (2002), have pointed out that there are combinations of V_p , V_s and pair with the soil skeleton Poisson ratio ν'_0 can be solved only in terms of complex numbers.

However, within the range of CH tests data base covered by the Author ($100 \leq V_s \leq 550$ m/s; $1500 \leq V_p \leq 3500$ m/s) in combination with $0.15 \leq \nu'_0 \leq 0.25$, the use of Foti *et al.* (2002) formula has, so far, yielded a solution in terms of real numbers.

This holds also for the data reported in Fig. 26, where the Foti's formula, although well posed, has yielded results conflicting with the comprehensive and reliable set of e_0 values determined in laboratory [Chandler *et al.* (2011)].

The evidence that the error on measured seismic waves velocity for the range of V_p and V_s considered in Fig. 27, amplifies by three times the error on the computed n_0 , has triggered the attempt to explore the intrinsic variability of V_p and V_s measured during 9 state-of-the-art CH tests recently carried out at the Zelazny Most site copper tailings, mentioned in Section 3 of this paper.

The following testing program has therefore been set up:

- In each CHT, at 1 m intervals, the seismic waves (V_p and V_s) velocity measurements have been repeated 10 times and the obtained values stored.
- In each in-hole a survey of the deviation from the verticality and of its azimuth has been carried in both in down-hole and up-hole modes repeating all the measurements three times at depth intervals of 3 m.

The bulk of the collected data will be used for the statistical and probabilistic evaluation of how the combination of the two independent variables, *time* and *distance*, affect the accuracy of measured V_p and V_s in the high quality CH tests.

The following preliminary information arising from the above tests can, currently, be anticipated:

- Figures 28 and 29, besides two CH tests results, report the standard deviation values of V_p and V_s measured ev-

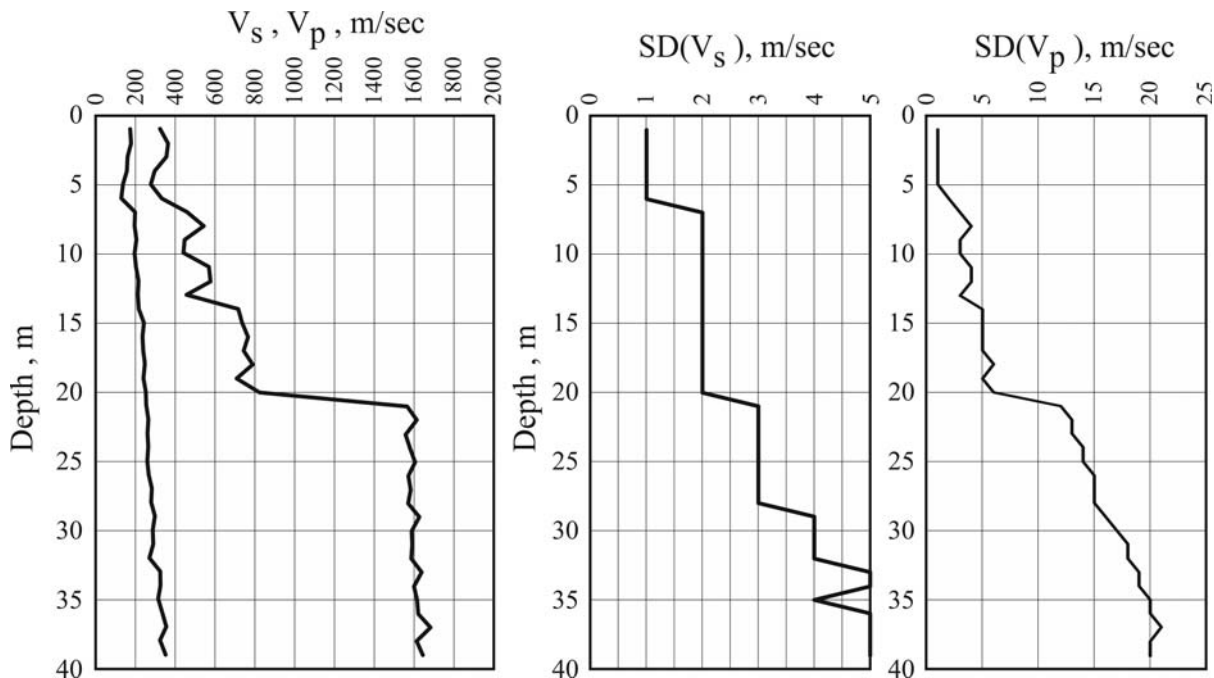


Figure 28 - Zelazny Most, North dam-CH 1-2, standard deviation of V_p and V_s after 10 measurement replications at 1 m intervals.

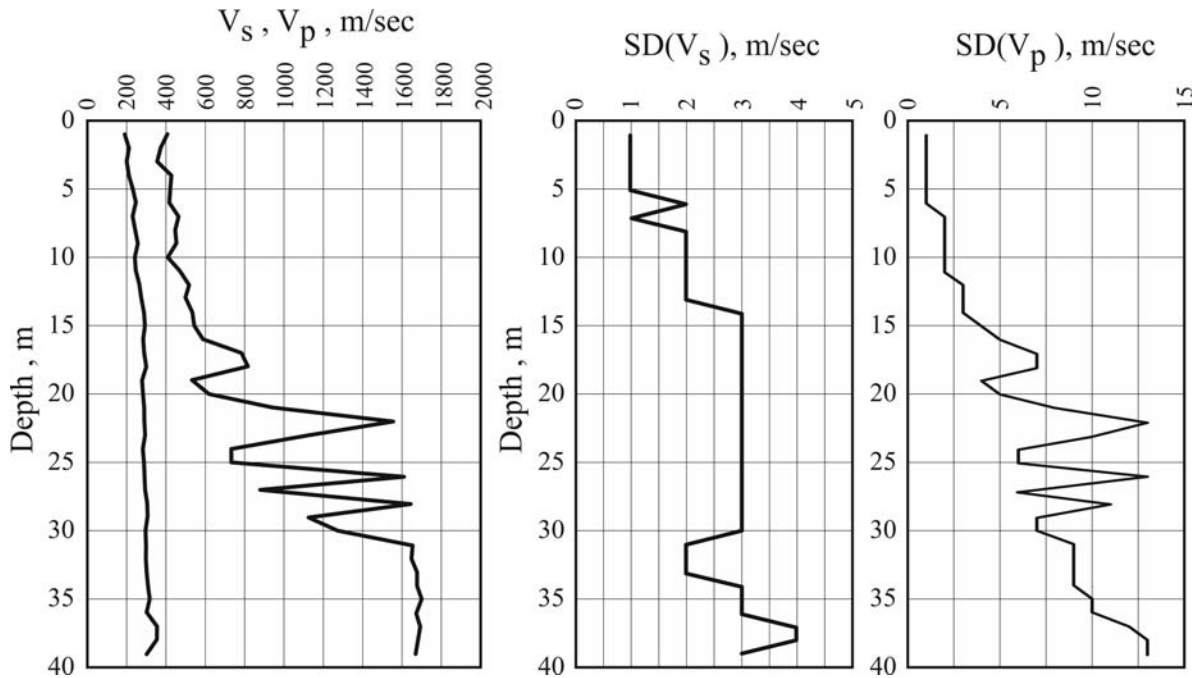


Figure 29 - Zelazny Most, North dam-CN 7-8, standard deviation of V_p and V_s after 10 measurement replications at 1 m intervals.

ery 1 m, computed from the data gathered after the ten-fold replications of the waves propagation.

- Figure 30 exemplifies how the variables uncertainties, *travel time* and *travel distance*, individually considered, affect the standard deviation and covariance of the measured V_p .

Figure 30 highlights the important evidence that, at least in the examined case, the uncertainty linked to the variable *travel distance* has a more significant impact than the *travel time* on the measured seismic waves velocity in CH tests reliability.

Thanks to its solid theoretical background, the formula by Foti *et al.* (2002) allows assessing e_0 and n_0 with the consistency most demanding engineering applications require, remarking that the hardware and software employed in CH and DH tests will be improved.

This work by Foti *et al.* (2002), offers a valid opportunity to estimate the porosity and the void ratio *in situ* of fully saturated soils from seismic body waves velocity measured in the field. However, when using this formula, which is yet to be validated, the following points should be considered:

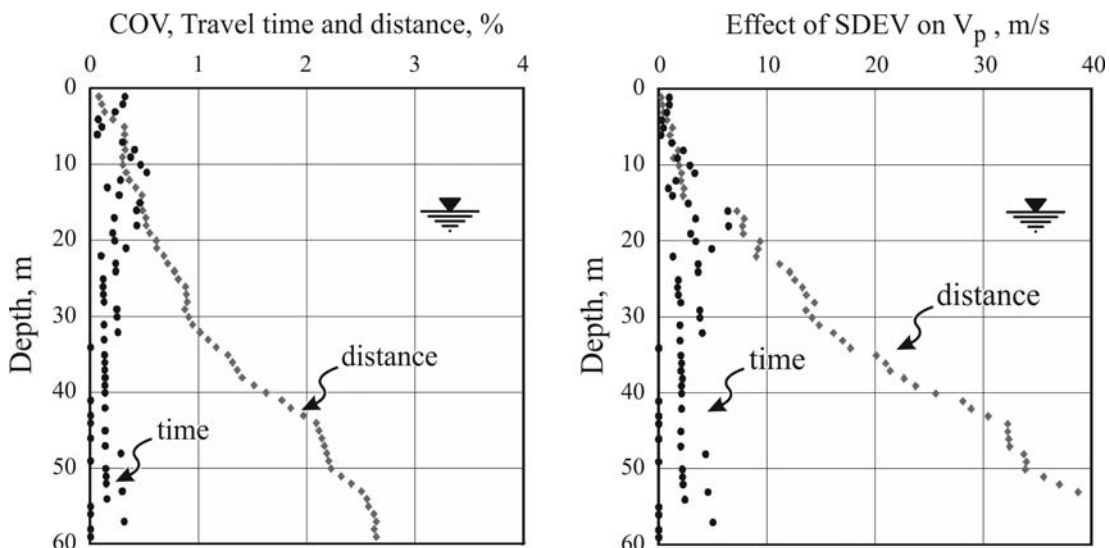


Figure 30 - Zelazny Most, P-waves arrival time and travel distance – Uncertainties involved.

- Dealing with the solution of an inverse problem, the computed value of porosity or void ratio is significantly affected by the accuracy and reliability of the measured seismic waves velocity. The above is especially relevant as regard the compression wave [Foti (2003)].
- However, the above issue, crucial when dealing with liquefaction and flow failure problems, becomes less significant in other engineering applications for which Foti *et al.* (2002) procedure, represents a step forward compared with the empirical correlations reliability between D_R and penetration tests results, used in common practice.
- A properly arranged and interpreted CH test is the most suitable mean to obtain independent, accurate V_p and V_s measurements to be used as input in the Foti *et al.* (2002) formula.
- As to Poisson coefficient ν_0 to be adopted when computing the porosity or the void ratio from V_p and V_s , it should be considered that the strains associated with the propagation of seismic waves is of the order of 10^{-6} at the best up 10^{-5} . At this strain level, the results of the large data base collected from the drained triaxial and plain strain tests with internal strains measurement, suggest values of ν_0 in the range between 0.15 and 0.25.
- The porosity and the void ratio computed using Foti *et al.* (2002) procedure, can be further enhanced if the uncertainties involved in assessing the picking arrival time and travel distance of V_p and V_s are accounted for.

6. Susceptibility of Coarse Grained Soils to Liquefaction

Since the pioneering work by Andrus & Stokoe (2000), the empirical approach to assess the susceptibility of sandy soils to cyclic liquefaction, based on the V_s measured in field, has been used in parallel with more conventional methods based on penetration tests results (SPT, CPTU, DMT). Figure 31 shows the correlation of V_{s1} vs. the

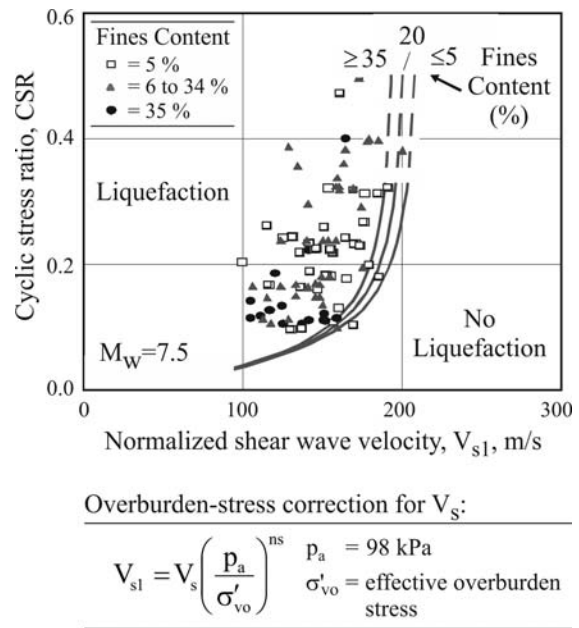


Figure 31 - V_s -based liquefaction susceptibility, Andrus & Stokoe (2000).

cyclic stress ratio (CSR) valid for an earthquake of $M_w = 7.5$ magnitude based on the analysis of the collected case records at locations where the cyclic liquefaction has been observed.

A comprehensive discussion and enhancement of the V_s procedure to estimate to what extent the coarse grained soil deposit is prone to liquefaction can be found in the book by Idriss & Boulanger (2008), who, in their discussion, raise the issue, already pointed out by Liu & Mitchell (2006), that V_s exhibits a lower sensitivity to variation of D_R *in situ* if compared to penetration tests.

The writer, referring to a large data base of more than 650 CPT DMT and seismic tests carried out in CC's on a variety of pluvially deposited dry sands, has attempted to explore the V_{s1} response to D_R changes as compared to those

Table 6 - V_s -sensitivity to D_R changes.

Calcareous oolithic Kenya sand				Siliceous Ticino sand			
D_R	p' (kPa)	V_s (m/s)		D_R	p' (kPa)	V_s (m/s)	
35%	100	175	$C_s = 238$	41%	100	119	$C_s = 90$
	200	212	$n_s = 0.27$		200	141	$n_s = 0.235$
	300	237	$d = 1.30$		300	155	$d = 1.30$
88%	100	230	$C_s = 275$	88%	100	191	$C_s = 110$
	200	278	$n_s = 0.25$		200	226	$n_s = 0.236$
	300	310	$d = 1.30$		300	247	$d = 1.30$
$V_s(D_R = 88\%) / V_s(D_R = 35\%) = 1.31$				$V_s(D_R = 88\%) / V_s(D_R = 41\%) = 1.60$			

$$V_s = C_s \left(\frac{p'}{p_a} \right)^{ns} \cdot \sqrt{F(e)} \quad F(e) = e^{-d}$$

Table 7 - CPT and DMT sensitivity to D_r changes.

D_r	CPT		D_r	DMT	
	p' (kPa)	q_c (m/s)		p' (kPa)	K_D (-)
30%	100	6.0	30%	100	1.77
	200	8.3		200	1.57
	300	10.0		300	1.45
60%	100	14.3	60%	100	3.52
	200	20.0		200	3.10
	300	24.0		300	2.89
$\frac{q_c(D_r = 60\%)}{q_c(D_r = 30\%)} = 2.4$			$\frac{K_D(D_r = 60\%)}{K_D(D_r = 30\%)} = 2.0$		

of CPT cone resistance q_c and of the Marchetti's DMT lateral stress index K_D . The results for the crushable calcareous oolitic Kenya sand [Fioravante (2001)] and for the siliceous Ticino river sand [Bellotti *et al.* (1996), Jamiolkowski *et al.* (2001)] are shown in Tables 6 and 7.

Comparing the results reported in Table 6 with those in Table 7 it can be confirmed the minor sensitivity of V_{s1} to D_r changes with respect to those of q_c and K_D . It is worthy to recall the readers' attention, that this difference is even more pronounced if the different range of D_r considered in the compilation of Tables 6 and 7 is accounted for. The brief mention to V_s used to assess the susceptibility of sandy soils to cyclic liquefaction allows the following comments:

The CC tests results on two dry sands confirm the lower capability of shear waves to respond to D_r changes if compared to the CPT- q_c and the DMT- K_D . This happens despite V_s , similarly to q_c and K_D , is function of *in situ* void ratio and effective stresses. Moreover, differently from all the penetration tests, since V_s measurements are less invasive than penetration tests, are more prone to be affected by some depositional and post-depositional phenomena as aging, cementation and cyclic pre-straining.

In the light of the above, the use of V_s should continue to evaluate the liquefaction potential, although subject to further laboratory and field validations. The current state of such method development offers the advantage of an easy application in gravelly soils where the feasibility and reliability of the approaches based on penetration tests, in many circumstances, appear questionable.

References

Andrus, R.D. & Stokoe, K.H. (2000) Liquefaction resistance of soils from shear-wave velocity. *J. Geotechnical & Geoenvironmental Eng.*, ASCE, v. 126:11, p. 1015-1025.

Arroyo, M. & Greening, P.D. (2002) Phase and amplitude responses associated with the measurement of shear-wave velocity in sand by bender elements: Discussion. *Canadian Geotechnical J.*, v. 39:2, p. 483-484.

Arroyo, M.; Ferreira C. & Sukolrat J. (2007) Dynamic measurements and porosity in saturated triaxial specimens.

Ling, H.I.; Callisto, L.; Leshchinsky, D. & Koseki, J. (eds) *Soil Stress-Strain Behavior: Measurement Modeling and Analysis*. Springer, A.A. Dordrecht, The Netherland, p. 537-546.

ASTM (2008) D2845-08 Standard Test Method for Laboratory Determination of Pulse Velocities and Ultrasonic Elastic Constants of Rock, Conshohochon, PA, USA, 14 pp.

Bellotti, R.; Jamiolkowski, M.; Lo Presti, D.C.F. & O'Neill, D.A. (1996) Anisotropy of small strain stiffness in Ticino sand. *Gèotechnique*, v. 46:1, p. 115-131.

Biot, M.A. (1956) Theory of propagation of elastic waves in a fluid-saturated porous solid. Part 1. Low frequency range. *The Journal of the Acoustical Society of America*, v. 28:2, p. 168-178.

Brignoli, *e.g.*M.; Fretti, C.; Jamiolkowski, M.; Pedroni, S. & Stokoe, K.H. (1996) Stiffness of gravelly soils to small strains. *Proc. XIV Int. Conf. on Soil Mechanics and Foundation Engineering*, Hamburg, v.1, pp. 37-40.

Chandler, R.J.; Jamiolkowski, M.; Faiella, D.; Ridley, A.M. & Rocchi, G. (2011) Suction measurements on undisturbed samples of heavily overconsolidated clays. *Proc. XXIV Convegno Nazionale di Geotecnica*, Napoli, v. 1, pp. 361-374.

Cox, B.R. (2006), Development of a Direct Test Method for Dynamically Assessing the Liquefaction Resistance of Soils *In Situ*. PhD Dissertation, Texas University, Austin.

Cubrinovski, M. & Ishihara, K. (1999) Empirical correlation between SPT N-value and relative density for sandy soils. *Soils and Foundations*, v. 39:5, p. 61-71.

De Groot, D.J.; Lunne T. & Tjelta T.J. (2011) Recommended best practice for geotechnical site characterisation of cohesive offshore sediments. *Gourvenec & White*, (eds) *Frontiers in offshore Geotechnics II*. Perth Western Australia. Taylor and Francis Group, London, pp. 33-57.

Darendelli, M.B. (1991) Development of a new family of normalized modulus reduction and material damping curves. PhD Dissertation, University of Texas, Austin.

Dobry, R.; Ladd, R.S.; Yokel, F.Y.; Chung, R.M. & Powell, D. (1982) Prediction of pore water pressure buildup and liquefaction of sands during earthquakes. *Building Science Series 138*, National Bureau of Standards, U.S. Dept of Commerce, Washington, D.C., 168 pp.

Fioravante, V. (2000) Anisotropy of small strain stiffness of Ticino and Kenya sand from seismic wave propagation measured in triaxial testing. *Soils and Foundations*, v. 40:4, p. 129-142.

Fioravante, V.; Giretti, D.; Jamiolkowski, M. & Rocchi, G.F. (2012) Triaxial tests on undisturbed samples of gravelly soils from the Sicilian shore of Messina strait. Accepted for publication in the *Bulletin of Earthquake Engineering*.

Foti, S.; Lai, C.G. & Lancellotta, R. (2002) Porosity of fluid-saturated porous media from measured seismic wave velocities. *Gèotechnique*, v. 52:5, p. 359-373.

- Foti, S (2003) Personal communication.
- Foti, S. & Lancellotta, R. (2004) Soil porosity from seismic velocities. Technical note. *Gèotechnique*, v. 54:8, p. 551-554.
- Giretti, D.; Fioravante, V.; Jamiolkowski, M.; & Lopresti, D.C.F. (2012) Elastic stiffness anisotropy of Kenya carbonatic sand. Paper in preparation.
- Grozic, J.L.H.; Robertson, P.K. & Morgenstern, N.R. (1999) The behavior of loose gassy sand. *Canadian Geotechnical J.*, v. 36:3, p. 482-492.
- Grozic, J.L.H.; Robertson, P.K. & Morgenstern, N.R. (2000) Cyclic liquefaction of loose gassy sand. *Canadian Geotechnical J.*, v. 37:4, p. 843-856.
- Hight, D.W. & Leroueil, S. (2003) Characterization of soils for engineering purposes. Proc. Int. Workshop on Characterisation & Engineering Properties of Natural Soils, Balkema, Singapore, p. 255-360.
- Hofmann, B.A. (1997) *In situ* ground freezing to obtain undisturbed samples of loose sand for liquefaction assessment. PhD Dissertation, University of Alberta.
- Hoque, H. (1996) Elastic deformation of sands in triaxial tests. Doctor of Engineering Dissertation, The University of Tokyo.
- Hoque, E. & Tatsuoka, F. (1998) Anisotropy in the elastic deformation of material. *Soils and Foundations*, v. 38:1, p. 163-179.
- Huang, A.B.; Tai, Y.Y.; Lee, W.F. & Ishihara, K. (2008) Sampling and field characterization of the silty sand in Central and Southern Taiwan. Proc. 3rd International Conference on Geotechnical and Geophysical Site Characterization, Taipei, Taylor & Francis Group, London, pp. 1457-1463.
- Idriss, I.M. & Boulanger, R.W. (2008) Soil liquefaction during earthquakes. Earthquake Engineering Research Institute, MNO-12, Oakland.
- Ishihara, K. (1996) *Soil Behaviour in Earthquake Geotechnics*. Clarendon Press, Oxford, UK, 350 pp.
- Ishihara, K.; Huang, Y. & Tsuchiya, H. (1998) Liquefaction Resistance of Nearly Saturated Sand as Correlated with Longitudinal Wave Velocity in Poromechanics: A Tribute to Maurice A. Biot. Balkema, Rotterdam, The Netherlands, p. 583-586.
- Ishihara, K.; Tsukamoto, Y. & Kamada, K. (2004) Undrained behaviour of near-saturated sand in cyclic and monotonic loading. Proc. International Conference on Cyclic Behaviour of Soils and Liquefaction Phenomena, Bochum, p. 27-40.
- Jardine, R.J. (1992) Some observations on the kinematic nature of soil stiffness. *Soils and Foundations*, v. 32:2, p. 111-124.
- Jamiolkowski, M.; Lo Presti, D.C.F. & Manassero, M. (2001) Evaluation of relative density and shear strength of sands from CPT and DMT Soil Behaviour and soft ground construction. ASCE GSP no. 119, p. 201-238.
- Jamiolkowski, M.; Ricceri, G. & Simonini, P. (2009) Great Project Lectures: Safeguarding Venice from high tides: site characterization & geotechnical problems. Proc. XVII ICSMGE, Alexandria, v. 4, p. 3209-3227.
- Jamiolkowski, M.; Carrier, W.D.; Chandler, R.J.; Hoeg, K.; Swierczynski, W. & Wolski, W. (2010) The geotechnical problems of the second world largest copper tailings pond at Zelazny Most, Poland. Dr. Za-Chieh Moh Distinguished Lecture. Keynote Speech I, VII Southeast Asian Geotechnical Conf. Taipei, v. 2, pp. 12-27.
- Jovicic, V.; Coop, M.R. & Simic, M. (1996) Objective criteria for determining $G_{(max)}$ from bender element tests. *Geotechnique*, v. 46:2, p. 357-362.
- Kokusho, T. (2000) Correlation of pore-pressure B-value with P-wave velocity and Poisson's ratio for imperfectly saturated sand or gravel. *Soils and Foundations*, v. 40:4, p. 95-102.
- Kuwano, R. & Jardine, R. (2002) On the applicability of cross-anisotropic elasticity to granular materials at very small strains. *Gèotechnique*, v. 52:10, p. 727-749.
- Lai, C.G. & Crempien de la Carrera, J.G.F. (2012) Stable inversion of measured V_p and V_s to estimate porosity in fluid-saturated soils. *Gèotechnique*, v. 62:4, p. 359-364.
- Landon, M.M.; DeGroot, D.J. & Sheahan, T.C. (2007) Nondestructive sample quality assessment of a soft clay using shear wave velocity J. *Geotechnical & Geoenvironmental Eng.*, ASCE, v. 133:4, p. 424-432.
- Lee, N.K.J. (1993) Experimental Study of Body Wave Velocities in Sand Under Anisotropic Conditions. PhD Thesis, University of Texas, Austin.
- Lee, S.H. (1985) Investigation of Low-Amplitude Shear Wave Velocity in Anisotropic Material. PhD Thesis, University of Texas, Austin.
- Lee, S.H. & Stokoe K.H. (1986) Investigation of low-amplitude shear wave velocity in anisotropic material. Report GR 86-6. University of Texas, Austin.
- Lee, S.J.; Cho, G.C. & Santamarina, J.C. (2005) Liquefaction: strength and wave based monitoring. First Japan-US Workshop on Testing Modeling and Simulation in Geomechanics. Boston, 2003, ASCE GSP no. 143, p. 463-474.
- Lewis, M.D. (1990) A Laboratory Study of the Effect of Stress State on the Elastic Moduli of Sand. PhD Thesis, University of Texas, Austin.
- Liu, N. & Mitchell, J.K. (2006) Influence of non plastic fines on shear wave velocity-based assessment of liquefaction. *J. Geotechnical & Geoenvironmental Eng.*, ASCE, v. 132:8, p. 1091-1097.
- Lo Presti, D.C.F. & O'Neill, D.A. (1991) Laboratory investigation on small strain modulus anisotropy in sand. Proc. First International Symposium on Calibration Chamber, ISOCCT1 Potsdam, p. 213-224.
- Lo Presti, D.C.F. (1991) Discussion on threshold strain in Soil. Proc. X European Conference on Soil Mechanics and Foundation Engineering, Firenze, v. 4, p. 1282-1283.
- Lo Presti, D.C.F. (1991a) Discussion on behaviour of sand at small strain. Proc. X European Conference on Soil

- Mechanics and Foundation Engineering, Firenze, v. 4, p. 1229-1230.
- Love, A.E.H. (1927) A Treatise on the Mathematical Theory of Elasticity. Cambridge University Press, Cambridge (reprinted by Dover Publication Inc. 1944).
- Lunne, T.; Berre, T. & Strandvik, S. (1997) Sample disturbance effects in soft low plastic Norwegian clay. Proc. International Symposium on Recent Developments in Soil and Pavement Mechanics, Rio de Janeiro, p. 81-102.
- Lunne, T.; Berre, T.; Andersen, K.H.; Strandvik, S. & Sjørusen, M. (2006) Effects of sample disturbance and consolidation procedures on measured shear strength of soft marine Norwegian clays. Canadian Geotechnical J, v. 43:7, p. 726-750.
- Menq, F.Y. (2003) Dynamic Properties of Sandy and Gravely Soils. PhD Dissertation, The University of Texas, Austin.
- Maqbooll, S.; Koseki, J. & Sato, T. (2004) Effect of compaction on small strain Young's moduli of gravel by dynamic and static measurements. Bulletin of Earthquake Resistant Structure, Research Centre no. 37, p. 41-50.
- Nakazawa, H.; Ishihara, K.; Tsukamoto, Y. & Kamata, T. (2004) Case studies of liquefaction of imperfectly saturated soil deposits. Proc. International Conference on Cyclic Behaviour of Soils and Liquefaction Phenomena, Bochum, p. 295-304.
- Pennington, D.S.; Nash, D.F.T. & Lings, M.L. (2001) Horizontally mounted bender elements for measuring anisotropic shear moduli in triaxial clay specimens. ASTM Geotechnical Testing J, v. 24:2, p. 133-144.
- Rahtje, E.M.; Chang, W.J.; Stokoe, K.H. & Cox, B.R. (2004) Evaluation of ground strain from *in situ* dynamic testing. 13th World Conf. on Earthquake Engng., Vancouver, paper 3099, 15 p.
- Ridley, A.M. & Burland, J.B. (1993) A new instrument for the measurements of soil moisture suction. Géotechnique, v. 43:2, p. 321-324.
- Roesler, S.K. (1979) Anisotropic shear modulus due to stress anisotropy. J. Geotechnical Eng., ASCE, v. 105:GT7, p. 871-880.
- Sanchez-Salinero, I.; Roesset, J. & Stokoe, K.H. (1986) Analytical studies of body wave propagation and attenuation. Geotechnical Engineering Report GR86-15, University of Texas, Austin, 348 pp.
- Sasitharan, S.; Robertson, P.K. & Sego, D.C. (1994) Sample disturbance from shear wave velocity measurements. Canadian Geotechnical J., v. 31:1, p. 119-124.
- Schmertmann, J.H. (1978) Guidelines for Cone Penetration Test Performance and Design. US Dept of Transportation, FHWA, R78-209, Washington, D.C. USA, p. 151.
- Skempton, A.W. (1954). The pore pressure coefficients A and B. Géotechnique, v. 4:4, p. 143-147.
- Skempton, A.W. (1961) Horizontal stresses in an overconsolidated Eugene clay. Proc. V Int. Conf. on Soil Mechanics and Foundation Engineering, Paris, v. 1, pp. 351-357.
- Skempton, A.W. (1986) Standard penetration tests procedures and the effects in sands of overburden pressure, relative density, particle size, ageing and overconsolidation. Géotechnique, v. 36:3, p. 425-447.
- Stokoe, K.H.; Lee, J.N.K. & Lee, S.H.H. (1991) Characterization of soil in calibration chambers with seismic waves. Proc. First International Symposium on Calibration Chamber, ISOCCT1, Potsdam, p. 363-376.
- Stokoe, K.H. II (2011) Seismic measurements and geotechnical engineering. 47th Terzaghi Distinguished Lecture, presented at Geo-Frontiers 2011, Geo-Institute National Meeting, ASCE, Dallas, March 15, 2011 to be published.
- Takahashi, H.; Katazume, M.; Ishibashi, S. & Yamawaki, S. (2006) Evaluating the saturation of model ground by P-wave velocity and modelling of models for a liquefaction study. International Journal of Physical Modelling in Geotechnics, v. 6:1, p. 13-25.
- Tsukamoto, Y.; Ishihara, K.; Nakazawa, H.; Kamada, K. & Huang, Y. (2001) Resistance of partly saturated sand to liquefaction with reference to longitudinal and shear wave velocities. Soils and Foundations, v. 42:6, p. 93-104.
- Valle Molina, C. (2006) Measurements of V_p and V_s in Dry, Unsaturated and Saturated Sand Specimens with Piezoelectric Transducers. PhD Dissertation, University of Texas, Austin.
- Valle Molina, C. & Stokoe, K.H. (2012) Seismic measurements in sand specimens with varying degrees of saturation using piezoelectric transducers. Canadian Geotechnical J., v. 49:6, p. 671-685.
- Viggiani, G. & Atkinson, J.H. (1995) Stiffness of fine-grained soil at very small strains. Géotechnique, v. 45:2, p. 249-265.
- Vucetic, M. (1994) Cyclic threshold shear strains in soils. Journal of Geotechnical Engineering, ASCE, v. 120:12, p. 2208-2228.
- Yoshimi, Y.; Hatanaka, M. & Oh-Oka, H. (1978) Undisturbed sampling of saturated sands by freezing. Soils and Foundations, v. 18:3, p. 59-73.
- Yoshimi, Y. (2000) A Frozen Sample of Sand That Did Not Melt, Proc. of GEOTECH – YEAR 2000. Developments in Geotechnical Engineering. Balasubramaniam, A.S. & Bergado, D.T. (eds) Asian Institute of Technology, Bangkok, v. 1. pp. 293-295.
- Weston, T.R. (1996) Effects of Grain Size and Particle Distribution on the Stiffness and Damping of Granular Soils at Small Strains. MS Thesis, University of Texas, Austin.
- White, J.E. (1965) Seismic Waves: Radiation, Transmission and Attenuation. McGraw-Hill Book Company, New York.